Sindy H. Wei
Ian Parker
Mark J. Miller
Michael D. Cahalan

A stochastic view of lymphocyte motility and trafficking within the lymph node

Authors' addresses
Sindy H. Wei[1], *Ian Parker*[2], *Mark J. Miller*[1], *Michael D. Cahalan*[1],
[1]Departments of Physiology and Biophysics, University of California, Irvine, CA, USA.
[2]Neurobiology and Behavior, University of California, Irvine, CA, USA.

Correspondence to:
Michael D. Cahalan
Departments of Physiology and Biophysics
University California-Irvine
D340 MED SCI I, 285 IH
Irvine, CA 92697-4561
USA
Tel.: +1 949 824 7776
E-mail: mcahalan@uci.edu

Immunological Reviews 2003
Vol. 195: 136–159

Immunological Reviews
0105-2896

Summary: Two-photon microscopy is providing literal insight into the cellular dynamics of lymphoid organs and, guided by analysis of three-dimensional images, into mechanisms that underlie cell migration and antigen recognition *in vivo*. This review describes lymphocyte motility and antigen recognition in the native tissue environment and compares these results with a much more extensive literature on lymphocyte motility, signaling, and chemotaxis *in vitro*. We discuss the *in vitro* literature on dynamic aspects of lymphocyte motility, chemotaxis, and the response to antigen and present the view that random migration of lymphocytes may drive a stochastic mechanism of antigen recognition in lymphoid organs, rather than being guided by chemotaxis.

Introduction

Analyzing single-cell behavior: role of the tissue environment

T cells encounter multiple positive signals in order to generate an immune response. This process can be broken down into several distinct phases: positive selection in the thymus, the initial encounter with antigen in the lymph node, a signal transduction cascade that leads to altered gene expression, secretion of cytokines, cell proliferation, homing to inflammatory sites, induction of effector function upon restimulation with antigen, and induction of programmed cell death or memory cell formation. The molecular mechanisms that regulate these functions are under intensive investigation. At the cellular level, coordination of an immune response is mediated by direct ligand/receptor interactions between cells that contact each other and by secreted molecules that interact with receptors on target cells to elicit a variety of responses. At the organ and tissue level *in vivo*, homing and motility are essential aspects of the immune response. All of these events are influenced by factors in the native environment that are difficult, if not impossible, to reconstitute in experimental systems.

As the immune response is initiated by contact between antigen-presenting cells (APCs) and antigen-specific T cells,

responses of individual T cells can be heterogeneous, with some cells in a population responding and others not. Such heterogeneity applies even to T cell responses within an apparently homogeneous collection of T cells bearing a single T-cell receptor (TCR) specific for a particular epitope. Furthermore, at the subcellular level, signaling may take place in local domains within the cell, for example at the point of contact between T cells and APCs. Thus, it is of crucial importance to investigate the immune response using a single-cell approach to circumvent the limitations of population biochemistry that inherently blur individual cell responses. A variety of imaging techniques now provide the means to investigate signaling with a resolution that can detect single molecules, interactions between molecules, localized and global changes in second messenger activity, gene expression, cell migration, and dynamic interactions between cells.

Seeing inside lymphoid organs

Ideally, it would be advantageous and most relevant to investigate cellular interactions, signaling cascades, and effector function all in the *in vivo* context. Although the field is very far from this goal, recent advances in microscopy, development of new probes including a variety of indicator dyes and fluorescent proteins expressed in transgenic mice, and new experimental preparations have created exciting opportunities for the study of lymphocyte motility, chemotaxis, and antigen recognition in the physiological context of the tissue environment. In particular, two-photon laser microscopy has opened a new window to visualize the cellular dynamics of lymphocytes and APCs deep within lymphoid organs (1). This method has now been applied to isolated lymphoid organs including lymph node and spleen (2–5), tissue fragments that model thymic differentiation (6), and to an intravital preparation of the inguinal node in an anesthetized mouse (7). We have concentrated primarily on the behavior of naïve $CD4^+$ T cells from DO11.10 mice. T cells were labeled *in vitro* and adoptively transferred into control recipient animals or animals that had been challenged with antigen in an adjuvant system that promoted a robust immune response. We have also compared motility patterns of T and B lymphocytes. Real-time imaging capabilities enable the kinetics of the immune response to antigenic challenge to be tracked over a physiologically relevant time course. We review below the capabilities and limitations of optical techniques for functional imaging of the immune system, and we describe results gained by two-photon imaging of adoptively transferred dye-labeled lymphocytes within the lymph node.

Live-cell optical imaging techniques

Imaging cell structure and behavior within complex structures, such as the lymph node, inherently requires an imaging technique that can provide thin optical 'slices', which can then be processed to yield three-dimensional information. Resolution at a cellular and subcellular level can currently be obtained only with optical techniques: either by confocal microscopy (8) or by using the more recent technique of two-photon imaging (9).

In confocal microscopy, laser light focused from an objective lens is used to excite fluorescently labeled cells or structures, and the emitted fluorescent light is collected through a pinhole aperture that largely rejects all light except that originating at the focal spot (8). By raster scanning the laser spot, a two-dimensional plane can be imaged, and a stack of such planes can be acquired as the microscope is focused at small increments into the specimen to sample a three-dimensional volume. This process can be sequentially repeated to accumulate a time-lapse movie. However, confocal microscopy has two serious drawbacks for live-cell imaging in thick biological tissues. The first is that scattering of light by most tissues limits the depth of visualization to only a few tens of micrometers – barely skimming below the surface of even a small lymph node. Secondly, even though light is imaged only from the focal spot, the laser beam excites both exogenous fluorophore molecules and endogenous chromophores in cells above and below this plane (*Fig. 1*, left); resulting in accelerated dye bleaching and possible cell toxicity owing to photodamage and free radical formation.

Two-photon microscopy achieves the same optical sectioning effect as confocal microscopy, but utilizing a different optical principle that enhances depth penetration and minimizes photobleaching and phototoxicity (1). In brief, fluorophores are excited by near-simultaneous absorption of two infrared photons, rather than by a single photon of visible light. The energy of a photon decreases with increasing wavelength, so that the two infrared photons together provide comparable energy to a single blue photon, and a fluorophore such as fluorescein is thus excited and subsequently emits a green photon as it would during regular fluorescence. Although well established in theory for many years, applications of two-photon excitation have become practicable only recently, following the development of lasers able to emit astonishingly brief (femtosecond) pulses of light with instantaneous energies high enough to achieve two-photon excitation. The fundamental advantage of two-photon excitation for microscopy is that fluorescence is excited only at the focal spot of a laser beam focused by an objective lens, giving an inherent optical section

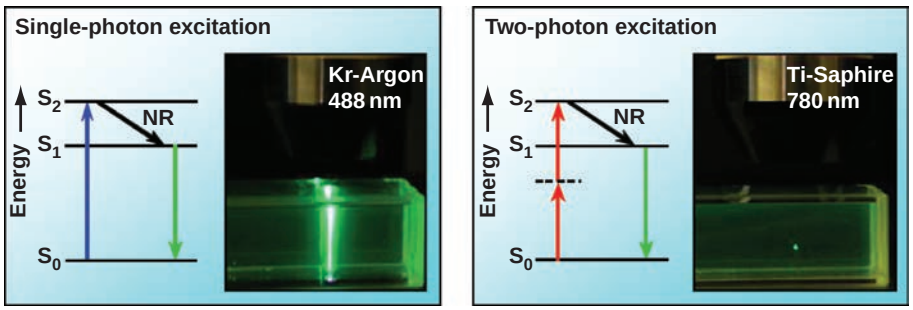

***Fig. 1.* Confocal versus two-photon excitation**. Confocal illumination (left) of fluorophore inside a cuvette excites fluorescence above and below the focal plane. Two-photon excitation (right) produces fluorescence only at the focal plane.

without the need to reject out-of-focus fluorescence (*Fig. 1*, right). This results because the requirement for almost simultaneous absorption of two photons means that fluorescence emission increases as the square (not linearly) with light intensity. Fluorescence is therefore great at the focal spot where photons are tightly compressed, but drops abruptly above and below this point as the laser beam diverges.

Two further advantages follow from this principle. The first is that excitation is achieved with infrared light, which being of relatively long wavelength penetrates tissues with much reduced scattering and thereby allows imaging more deeply (up to 500 μm) into biological specimens. The second advantage is that two-photon excitation (and hence photobleaching and photodamage) is largely confined to the focal plane: cells or subcellular regions above and below experience only the relatively innocuous infrared light.

Despite the aforementioned advantages, two-photon microscopy is not a universal solution to all live-cell imaging problems. As with any new technique, it has limitations and pitfalls that must be learned from experience. An important lesson is that two-photon excitation does not obviate problems of cell toxicity, but rather these problems arise under a different garb. Our experience (10) is that photodamage in both neurons and immune cells arises as a three-photon (or possibly higher) process, possibly involving excitation of cytochromes and similar molecules that absorb ultraviolet (UV) light. Thus, as the laser intensity at the specimen is progressively increased, the fluorescence increases as the square of intensity, but a threshold for cell damage (indicated by a Ca^{2+} rise in neurons and cessation of motility in lymphocytes) is abruptly reached, as this intensity increases steeply as a third-power function. This problem is exacerbated, because currently available cell tracker dyes and other probes were developed for use with conventional (one-photon) microscopy and require relatively high laser powers to give sufficient fluorescence emission with two-photon excitation. Consequently there is a fine dividing line between not being able to see cells, and killing them! Future improvements should be possible by the development of new fluorophores with improved two-photon absorption cross-sections and by optimization of microscope objectives and detector light paths to maximize collection of emitted fluorescence photons.

Another limitation is that, although providing a big improvement over confocal microscopy, the depth to which two-photon images can be acquired into tissues remains restricted to a few hundred microns. For example, we are able to image clearly only to a depth of about 300 μm into lymph nodes, providing limited axial window to view DCs that are typically found >200 μm below the capsule. One problem is that increased scattering results in a dimming with increasing depth into a tissue, but this dimming can be readily compensated for merely by increasing the laser intensity. Indeed, when purchasing a two-photon system, it may be advantageous to specify the most powerful laser available, because, given unavoidable losses in the scanning system and microscope optics, surprisingly high (>1W) laser powers are required. A more fundamental problem is the degradation of image quality at increasing depths, which arises even with water-immersion objectives that eliminate problems of spherical aberration. This degradation probably arises in large part because irregular variations in the refractive index within the tissue distort the wavefront of the laser beam. For example, a thin layer of adipose tissue above a lymph node greatly compromises image quality and imaging depth, likely because lipid droplets act as myriad 'microlenses'. Such extraneous tissue can, of course, be readily removed, but distortion within the actual tissue being imaged is more difficult to correct. In this regard, applications of adaptive optics (borrowed from astronomy) to scanning microscopy may offer a partial solution (11).

Biological preparations for lymphoid tissue imaging

The ideal goal is obviously to image the behavior of single immune cells within their undisturbed environment in an intact living animal. Although considerable progress has been made toward this end, most studies to date have utilized

technically easier preparations of explanted intact organs (*Fig.* 2) (2–5). These investigations maintain the structural integrity of the native tissue, but they have obvious limitations in that the normal vascular and lymphatic circulations are severed. A further issue concerns the appropriate maintenance of oxygen tension within lymphoid tissue. Lymph nodes are highly vascularized and metabolically active and, by analogy with long-standing practice for recording from brain slices, we reasoned that it would be important to optimize oxygenation of explanted nodes by superfusing them with solution equilibrated with 95% O_2/5% CO_2. This decision was also prompted by our initial attempts to image nodes that had been gently pressed against a microscope coverglass so as to permit the use of oil-immersion objectives. T cells in regions under the coverglass were often found to be immotile, whereas peripheral regions more directly exposed to the flow of superfusion fluid showed highly active cells, suggesting that the stationary cells were anoxic. On the contrary, it has been proposed that the normal oxygen tension in lymph nodes may be low (3, 12, 13), and that lymphocyte motility is unphysiological when nodes are superfused with 95% O_2. However, recent experiments (7) using intravital imaging showed that T-cell motility in lymph nodes of a live mouse (whether breathing room air or 95% O_2/5% CO_2) was similar to that in our explanted node preparation. These findings validate the use of explants to study T-cell motility under appropriate conditions.

Our development of an intravital imaging technique (7) required that a lymph node be isolated, mechanically stabilized and maintained at appropriate temperature, while avoiding any interruption of normal blood and lymphatic circulation. Thus far, we have achieved this goal with inguinal lymph nodes of the mouse, which can be readily accessed by folding back a broad flap of abdominal skin. A rubber O-ring is glued onto the inner surface of the exposed skin flap with tissue adhesive (Vetbond, 3M Corp.) and stabilized by fitting it into a rigidly mounted Plexiglas surround. The O-ring and surround form a watertight chamber filled with phosphate-buffered saline (PBS), into which a water-dipping objective is lowered for imaging. Both the mouse and the chamber are warmed, and the temperature in the chamber is independently maintained at 35–36 °C. To avoid impeding circulation, the O-ring is not pressed down onto the skin flap, but is laterally stabilized to prevent movement artifacts from respiration. Bright field imaging of erythrocyte flow readily confirms that the blood circulation is not impaired, and pulse-related movement artifacts are usually minimal (*c.* 1 μm) provided that the node is left supported by a surrounding layer of adipose cells (*Fig.* 3).

Motility of T and B cells in lymph node

Two-photon imaging of fluorescently labeled lymphocytes provides a means of visualizing their native behaviors and motilities within the natural environment of lymph nodes and other lymphoid tissue. By taking a series of optical sections at small increments into the tissue, it is possible to build time-lapse movies, imaging cells as they move in three dimensions. The initial impression when viewing such movies is that labeled T cells and B cells are 'swimming' freely in an apparently open and unobstructed medium. In reality, of course, that is not the case. Within the node, there is a great excess of

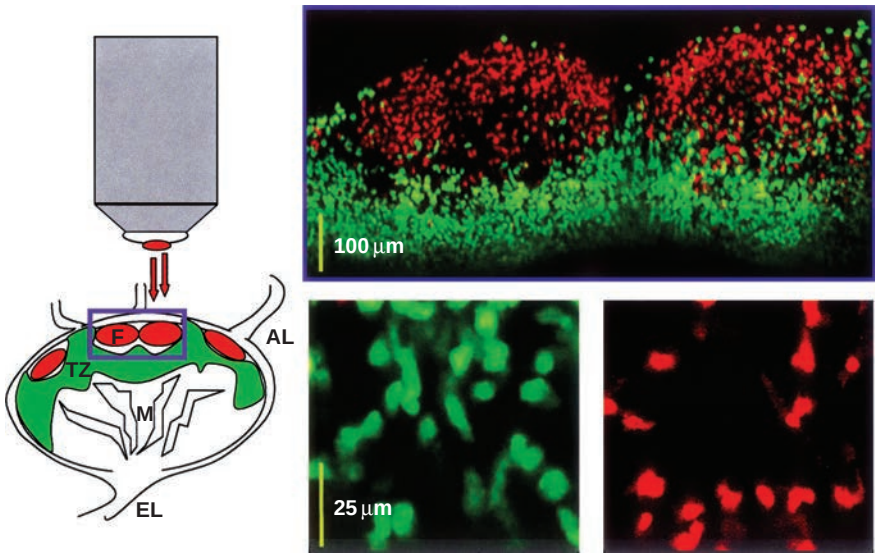

***Fig.* 2. Imaging living T and B cells inside the lymph node**. A lymph node explant can be imaged at different magnifications to reveal defined compartments of B-cell (red) follicles (F) and cortical T-cell (green) regions (TZ). EL, AL and M represent the efferent and afferent lymphatics and the medulla, respectively. The image represents a cross-section of the three-dimensional volume of the lymph node. The motile behavior of individual cells within these regions can be tracked by time-lapse recording. Similar image as in (2).

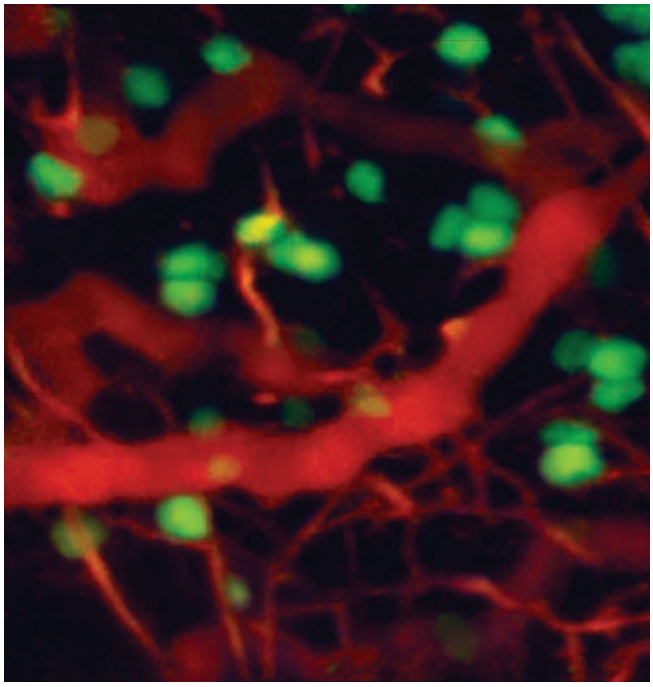

***Fig. 3.* Intravital imaging in the inguinal node**. T cells and high endothelial venule (HEV), along with the reticular fiber network, are visualized in the intact lymph node by labeling with fluorescent dyes. Intravital preparations permit the study of homing and possible chemotaxis by preserving lymphatic and blood vessels. Similar image as in (7).

'invisible' unlabeled lymphocytes and other motile cells. Moreover, reticular fibers form a rigid scaffold within the node, which is also threaded by fixed structures such as blood vessels. The movements of lymphocytes thus depend both on their intrinsic motility and on passive collisions and active interactions with surrounding cells and structures.

Random walks and diffusion

Despite this complexity, a remarkable finding is that the aggregate motions of both T cells and B cells, visualized over tens of minutes, closely approximate to a random walk pattern. Such behavior was first analyzed for phenomena such as diffusive motion of molecules and Brownian motion, where thermal energy provides the impetus for the motion. Here, a particle is constantly bombarded by other molecules and is moving in a succession of tiny random steps. A defining characteristic is that the particle at first moves rapidly away from any given starting point but may then partly backtrack, so that its absolute displacement from the starting point increases at a progressively slower rate at increasing times. Although the motions of any individual particle are random, the average behavior of numerous particles is entirely predictable. An important result is that the mean displacement from the origin grows as a square-root function of time. For example, a particle may move a mean distance of 1 μm in 1 ms, but it would take on average 100 ms to move 10 μm and 10 s to move 100 μm. This relationship is defined by a single parameter, the diffusion coefficient D, such that the mean distance d traveled in time t is given by:

$$d = \mathrm{sqrt}(6Dt)$$

The proportionality factor of 6 applies for diffusion in three dimensions. For diffusion in two dimensions (on a planar sheet) the factor is 4 and for one dimension (along a line) the factor is 2. The unit of the diffusion coefficient is $\mu m^2\, s^{-1}$. Diffusion is often considered in situations where there is an initially high concentration of particles (e.g. a droplet of dye molecules introduced into a large volume of water) in one region, creating a concentration gradient. A common misconception is that some 'force' is exerted on each molecule, tending to make it move in a net direction down the concentration gradient. This is not the case. Each individual dye molecule experiences no force and moves randomly without influence from other molecules. Dissipation of the concentration gradient arises because all molecules start from approximately the same position and will thus move randomly away, whereas there are few dye molecules at distant locations that might randomly move back to the starting point.

Lymphocyte motility

The situation with lymphocytes moving within a tissue is analogous to such Brownian motion but involves very disparate mechanisms. Most significantly, lymphocytes display intrinsic locomotion through cytoskeletal rearrangement. This engine is the main cause of movement. It seems that collisions by neighboring cells cause little movement, because cells that have rounded and become immotile display only slight 'jiggles' of a few microns.

T cells progress by a series of repetitive lunges, repeatedly balling-up and then extending. This cycle appears to be driven by an intrinsic rhythmicity, with a period of about 2 min. During each cycle, the cell progresses an average distance of about 20 μm. Peak velocities reach as high as $25\,\mu m\,min^{-1}$ but, taking into account the pauses when it is almost stationary, the mean velocity of T cells (at 36 °C) along their meandering path is about $12\,\mu m\,min^{-1}$. T cells travel in a fairly consistent direction during each 'lunge' and may even continue in a consistent direction over several cycles. However, following each pause, there is a high probability that a cell will take off in another direction. Thus, tracks of T cells display a random walk pattern when followed over long times

encompassing many motility cycles, even though motions at short times are more linear.

A useful concept here, borrowed again from diffusion analysis, is that of a mean free path length. In the case of molecular diffusion, this length is the (extremely short) distance a molecule will travel in a straight line before being deflected by collision with another molecule. For T cells, the mean free path length is set by the interval between abrupt turns, resulting in a mean length of about 20 μm. When a T cell is tracked, it therefore initially moves in a fairly consistent direction, at a velocity of about 10 $\mu m\,min^{-1}$, but then begins to turn randomly so that its displacement from any given point of origin increases ever more slowly. *Fig.* 4 illustrates typical tracks superimposed from several T cells.

For times longer than about 4 min, the mean displacement of T cells swimming within a lymph node follows the square-root of time function expected for a random walk (*Fig.* 4). We have characterized the slope of this function as a 'motility coefficient', analogous to the diffusion coefficient. For naïve T cells at 36 °C in a lymph node, this value is about 67 $\mu m^2\,min^{-1}$. Thus, T cells will move an aggregate distance of about 10 μm in 24 s, 100 μm in 40 min and 1 mm in 66 h.

B cells display motility that is characteristically different to T cells. Whereas T cells advance by a series of lunges with cyclically varying velocity, B cells move at a more consistent though slower (*c.* 6 $\mu m\,min^{-1}$) velocity and appear to 'feel out' their environment by probing with amoeboid-like processes. Nevertheless, their aggregate behavior can again be described well as a random walk, with a motility coefficient of about 12 $\mu m^2\,min^{-1}$.

Autonomous randomly directed T- and B-cell trajectories

In the absence of specific antigen, we have examined the motility of wildtype T cells, naïve transgenic $CD4^+$ T cells, and B cells within their respective compartments (2, 7). An analysis of their motion failed to detect any evidence for directed motion amidst the blur of cells rapidly migrating in an apparently autonomous manner along randomly oriented trajectories. In both the explanted lymph node and *in vivo* in the inguinal lymph node intravital two-photon preparation, T cells again migrated randomly without evidence for directed motion (*Fig.* 4). At sites of homing, migration of T cells immediately subsequent to extravasation also was randomly directed (7). Although chemokines undeniably regulate T-cell motility, our 3D tracking results indicate that T cells migrate autonomously in the T-cell area and B cells likewise in the follicle, providing no evidence for the directional guidance of putative chemokine gradients. Observation of T and B cells at the follicle border also did not reveal evidence of chemotaxis; instead, cells behave as if encountering a physical obstacle or a highly localized substrate boundary (*Fig.* 5; see also video in *Supplementary material*).

Stochastic detection of antigen

An APC faces a 'needle in a haystack' problem of how to encounter that rare (one in a million) T cell with appropriate antigen specificity. To accomplish this task in the expanse of the T-cell zone, chemokine gradients emitted by DCs might assist the T cell to locate its target; if so, T cells would be expected to congregate near DCs (*Fig.* 6, left). Such a mechanism would recruit both antigen-specific and non-specific T cells, with the potential drawback that competition for space at the DC might then limit access to antigen. Our observations of

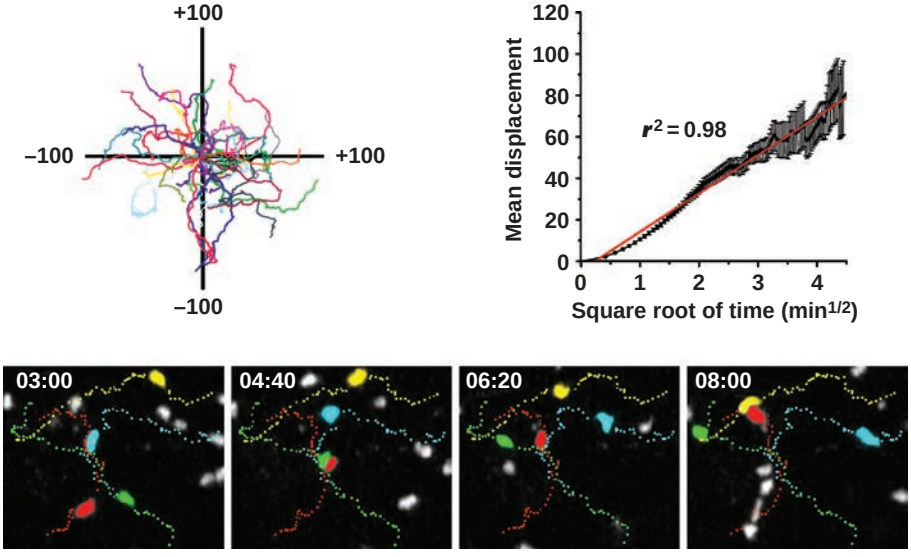

***Fig.* 4. T-cell movement *in vivo*.** In an intravital preparation of inguinal node, T cells exhibit no preference for any direction of travel, as shown by individual trajectories normalized to the origin (left). Analysis of the mean displacement with time suggests that cells move by a random walk (right). Time-lapse images of four T cells in the intravital lymph node. Each cell and its corresponding trajectory are color-coded. Reprinted from Millet MJ, et al. Proc Natl Acad Sci USA 2003;**100**:2604–2609.

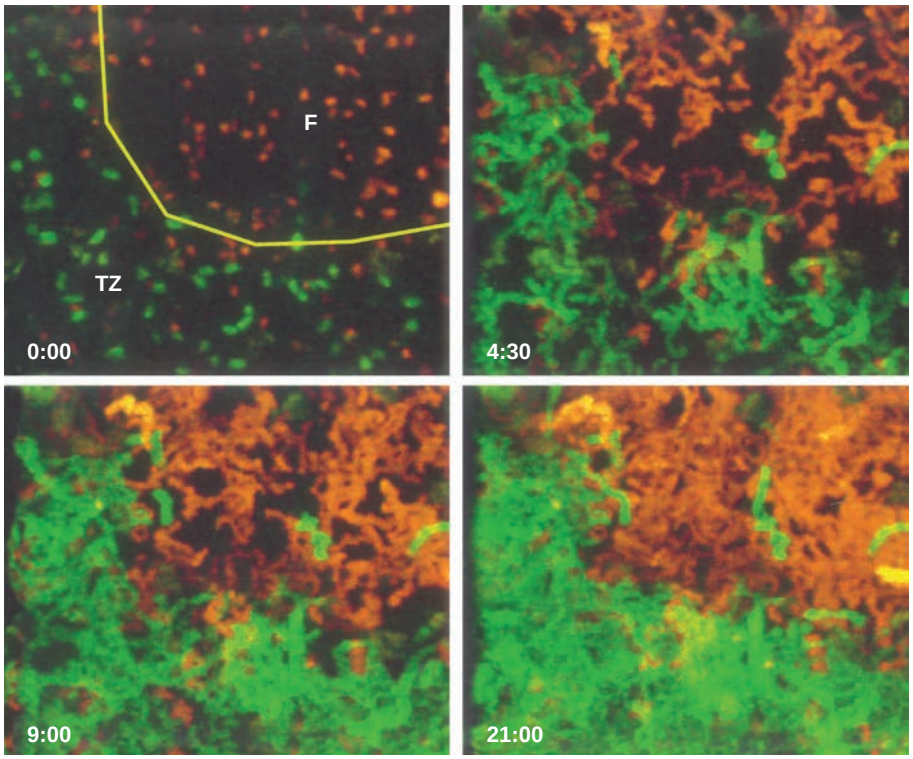

***Fig. 5.* Motion at the edge of a follicle.** T- (green) and B (red)-cell motion at the edge of a follicle (outlined in yellow). Images are accumulated sequentially in the four panels. See also video in *Supplementary material*.

robust and randomly directed T-cell motility in lymphoid tissue suggest that this process of T-cell/DC interaction is driven by random, autonomous motility of individual T cells (*Fig.* 6, right) (7). In the absence of antigen, naïve T cells appear to behave as individuals, migrating freely along separate paths without indication of directed motion along pervasive chemokine gradients or local congregation at specific sites.

Responding to antigen

During an immune response, T-cell behavior within the lymph node changes dramatically. Following antigen challenge, we observed an uneven distribution of T cells, and three separate patterns of motility were observed (*Fig.* 7) (2). Some cells moved rapidly along random paths. Others formed relatively stable clusters or T cells. Another group of cells moved in tight loops, giving the appearance of a swarm in a time-lapse video. The altered turning behavior of T cells may represent a modified program of random motility in which turns occur more frequently following contact with a DC. Cell proliferation could also be observed directly in lymph nodes 24 h after antigen challenge. Stalled out, enlarged T-cell blasts were seen dividing, giving rise to smaller cells with half the total quantity of label. Using carboxyfluoresein succinimidyl ester (CFSE) as an indicator of the number of cell divisions, we were able to demonstrate that T cells resumed a normal pattern of rapid motility following proliferation.

In vitro studies of lymphocyte motility, chemotaxis, and antigen presentation

Living cells within lymphoid organs have been imaged only within the last 2 years, compared with nearly 20 years of imaging studies employing *in vitro* approaches. Molecular studies have defined many elements of the signaling cascade that leads to lymphocyte activation, but several questions remain regarding molecular and cellular dynamics. What provides the initial TCR signal: receptor aggregation or a conformational change induced by peptide–major histocompatibility complex (MHC) complexes? How do molecules rearrange in the two-dimensional geometry of the membrane at the point of contact: passively by a diffusion trapping mechanism or actively via cytoskeletal rearrangements? What are the factors that regulate contact duration? Within the past 5 years, *in vitro* imaging studies have begun to reveal an intricate choreography of the key signaling molecules at the immunological synapse (IS). The synapse can be defined as an organized structure that provides communication between cells. The IS is a dynamic structure that forms and remodels with plasticity that may exceed anything observed in a neuronal synapse, with the possible exception of initial synapse formation during development. Our purpose here is to highlight certain aspects of cellular dynamics *in vitro* that point the way toward future *in vivo* studies.

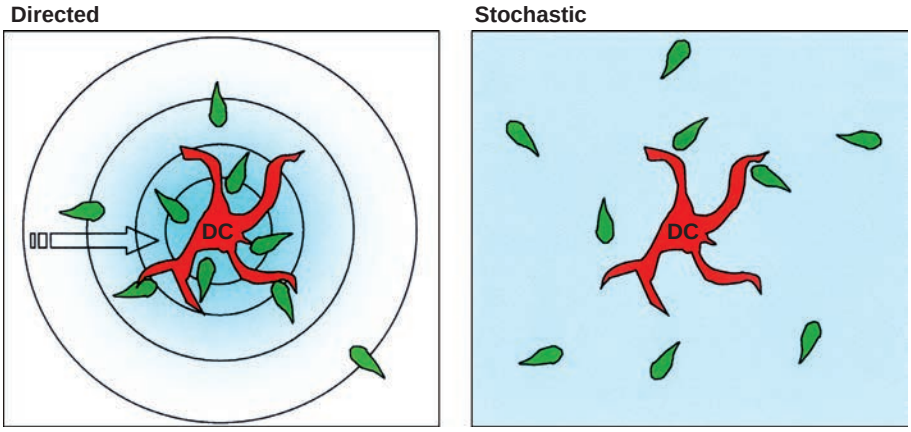

***Fig. 6.* Two models for T-cell/dendritic cell encounters**. Left, a gradient of chemokine attracts T cells. Right, T cells approach and encounter dendritic cells randomly.

Motility

Clearly, the ability to crawl on any substrate must represent a balance between adhesion and the ability to extend processes and move in a particular direction. If the surface is too sticky, then a cell rounds up or flattens out but cannot crawl; if the surface is not sticky enough, a cell cannot gain traction to move forward. Not surprisingly then, results on lymphocyte motility and interactions with APCs have given drastically differing results depending on the experimental system, making it difficult to extrapolate motility properties studied on artificial substrates *in vitro* to the *in vivo* setting. In most previous *in vitro* studies, T lymphocytes typically moved more slowly when plated on a two-dimensional substrate such as glass, compared with their velocity *in vivo* or in a three-dimensional collagen gel culture system (14–17). T cells crawl rapidly on intercellular adhesion molecule-1 (ICAM-1)-loaded lipid bilayers (18). On glass, activated T cells and an antigen-specific T-cell hybridomas exhibited polarized cell shape and were motile *in vitro*, but resting T cells did not adhere well and were unable to move at all (17). This difference between the resting and activated phenotype likely represents a change in substrate specificity for adhesion rather than an intrinsic change in the ability to move, since naïve T cells are highly motile in the lymph node (2). In addition to substrate, temperature is also clearly an important determinant of motility. Below *c.* 30 °C, lymphocytes move very slowly, if at all, either *in vivo* or *in vitro*. At elevated temperatures, patterns of movement were similar for antigen-specific T cells *in vivo* or *in vitro*. Regardless of substrate, T cells tend to move in an amoeboid manner, extending a veil of membrane at the leading edge during periods of motion and retracting the trailing edge, or uropod, periodically (17). Episodes of movement are interrupted by pauses when the cells round up; on average, periodicities of 1–5 min are observed on glass or in the lymph node (7, 17). In a collagen gel culture system, T cells also exhibited a stop-and-go temporal periodicity of motion (19). The stop-and-go pattern may be part of an intrinsic program of motility, but it is likely that this pattern can be modulated by factors encountered in the environment. Links between the cytoskeleton, motility, and antigen responsiveness have been discussed previously (20, 21).

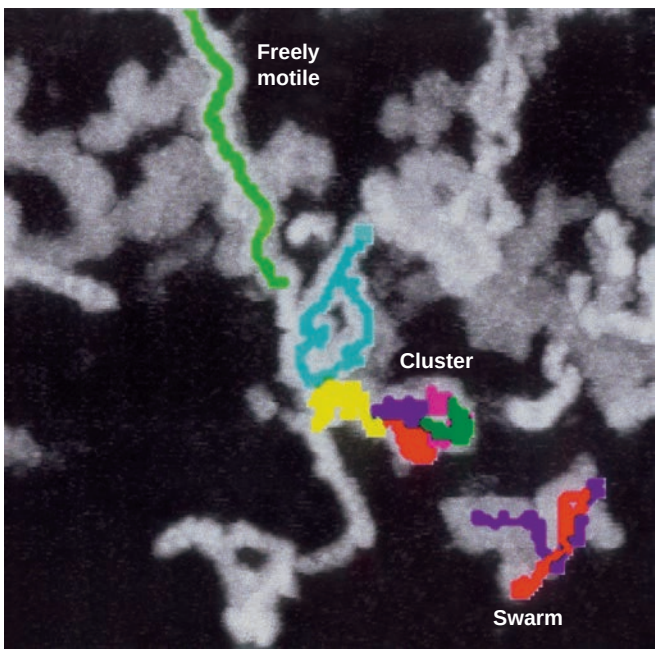

***Fig. 7.* T-cell behavior following antigen challenge.** A few individual cell tracks are shown superimposed upon accumulated images.

Chemotaxis

Chemokines and their receptors constitute a large family of proteins in humans (~50 and 20, respectively), which mediate chemotaxis and other functions, including extravasation of leukocytes and triggering of costimulatory or inhibitory signals (22–24). Chemokines bind to seven-transmembrane receptors coupled to G_i and activate phospholipase C and Ca^{2+}

signaling via a pertussis toxin-sensitive pathway (25–28). Extensive studies in bacteria, *Dictyostelium*, neuronal growth cones, and neutrophils provide convincing evidence of chemotactic motion directed by chemokines. For example, in *Dictyostelium* and in neutrophils, a mere 2% difference in chemokine concentration between the ends of a 10-μm long cell is sufficient to cause movement toward the source (29, 30). Great progress has been made in defining the extensive family of chemokines and their receptors in cells of the immune system, and chemokine gradients have been proposed to mediate processes such as constitutive trafficking through lymphoid compartments. However, unlike the well-defined cell systems mentioned above, there have been relatively few mechanism-based investigations on lymphocyte chemotaxis, and the existence of chemotactic gradients has yet to be definitively established in lymphoid tissue. Indeed as we discuss below, it has not even been firmly established whether lymphocytes exhibit chemotaxis, according to the original definition of the term.

In the 1880s, the term 'chemotaxis' was coined by Wilhelm Pfeffer to describe the observation that bacteria are able to swim towards or away from a stimulus and was later applied to indicate preferred directional migration of cells, including bacteria, spermatozoa, leukocytes, and ameba, along a chemical gradient. Chemotaxis can be defined as the ability of a cell to migrate toward a source of a chemoattractant molecule, i.e. movement up a concentration gradient. Negative chemotaxis, also termed chemofugetaxis, can cause movement away from a repulsive chemokine; in some cases a given molecule can exert positive or negative chemotaxis depending upon the conditions and cell type. Chemokinesis is the ability of a chemokine to cause an increase in random, not directed, motility. Haptotaxis represents movement up a chemokine gradient immobilized to a substrate. The distinctions among directional sensing, polarization, chemokinesis, haptotaxis, and chemotaxis are becoming more clear as the molecular mechanisms governing each process are further elucidated in other cell types (31).

Chemotactic mechanisms: lessons from other cell types

Mechanisms of sensing: temporal (sequential) versus spatial (simultaneous)

Cells that undergo chemotaxis are remarkably sensitive to small differences in concentration of chemoattractant over the cell length. Based on *in vitro* experiments, two major models have been proposed: spatial and temporal sensing. In many cases, both may be involved simultaneously. Spatial sensing is likely more important in stationary cells, and it involves detecting differences in chemoattractant concentrations across the cell. The signal-to-noise hypothesis predicts that cell polarization will be randomly oriented with spatially uniform chemokine concentrations, but the cell will become increasingly oriented toward higher concentrations of chemokine in the presence of a gradient (32). Temporal sensing is thought to play a dominant role in the chemotaxis of small locomotory cells such as bacteria, where cells sense time-dependent changes in concentration as they move. With both mechanisms, receptor modification and downregulation are key adaptations to chemokine gradients that can prevent receptor saturation.

Dictyostelium discoideum

Early experiments on amoeboid chemotaxis focused on applying extracellular chemical agents to motile cells in order to elucidate the effects on morphology, polarity, and motility. One model system for the study of amoeboid chemotaxis is the cellular slime mold *Dictyostelium discoideum*, a lower eukaryote that responds to different chemotactic stimuli throughout different stages of its life cycle (33). In the unicellular stage of its life cycle, the ameba is attracted to a bacterial food source by secreted folic acid and related pterin (having a pteridine ring) compounds. Even though an experimental compound may cause chemotaxis, it is not necessarily the natural chemotactic component (34). Negative chemotaxis on the other hand helps to scatter cells to optimize the search for nutrients. Upon starvation, individual ameba begin a process of aggregation that begins with pulsatile secretion of the chemoattractant cyclic-3′5′adedonsine monophosphate (cAMP) to cells within >1 cm radius, which in turn stimulates chemotaxis, 'entrainment' of migrating cells to amplify the signal by secreting more cAMP, relay of the signal as described by successive waves radiating from the aggregation center, and finally the 'streaming' of cells in a linear fashion towards the center (34).

Dictyostelium possesses four G protein-coupled receptors (GPCR) cAR1–cAR4 (35) for extracellular cAMP that respond to chemotactic stimulation by initiating a cascade of events similar to that evoked by chemokines in leukocytes. Signaling begins with a temporary rise in phosphoinositides, cAMP, cyclic guanosine 5′monophosphate (cGMP), inositol-1,4,5, -trisphosphate (IP_3), intracellular Ca^{2+} and consequently, the activation of the actin cytoskeleton beginning with actin nucleation and modified by actin cross-linking proteins that aid in extension of pseudopodia and filopodia (36–38). A cytosolic regulator of adenylyl cyclase containing a pleckstrin homology domain was found to be essential to signal transduction. Upon ligand binding, it is recruited to

the membrane to regulate activation of adenylyl cyclase, possibly by its interaction with $G_{\beta\gamma}$ subunits (39, 40). Distribution studies of the cAR1-GFP fusion protein reveal uniform distribution of receptors after stimulation by a cAMP gradient (41). However, chemotaxis in these cells remained intact despite the absence of receptor polarization. The cytosolic regulator of adenylyl cyclase that is translocated to the membrane and redistributed to the site of pseudopod formation within the first 10–30 s after exposure to a gradient of cAMP. A uniform application of cAMP only stimulates homogenous recruitment of cytosolic regulator adenylyl cyclase to the membrane (32). Cytosolic regulator adenylyl cyclase translocation is followed shortly by phosphoinositide 3-kinase (PI3K) recruitment to and phosphatase and tensin homolog (PTEN) release from the membrane, leading to a local increase in synthesis and decrease of breakdown of phosphatidylinositol-3,4,5-triphosphate (PIP_3) (42). Polarization of components in the signaling apparatus may not provide proof of chemotactic ability because while the non-polarizable cAMP receptor and downstream G-proteins are necessary for chemotaxis, polarizable cytosolic regulator of adenylyl cyclase (CRAC) is not required (43, 44). Even though there is no preference for cAMP receptors for the leading edge, the receptors here bind and release ligand faster than receptors at the uropod due to other regulatory mechanisms (45).

Both spatial and temporal sensing have been supported by studies of chemotaxis in *Dictyostelium* (34), but Vicker *et al.* (46, 47) report that this organism could not detect the orientation of spatial gradients but requires a pulse or impulse of cAMP to induce chemotaxis (rather than klinokinesis, in which magnitude and frequency of turning behavior is altered or orthokinesis, in which speed or frequency of movement is increased). It has been shown that pretreatment of *Dictyostelium* (and neutrophils) with chemoattractant can rapidly lead to reduced receptor availability for binding the same substance, with a half life of 1–10 min (48–51). The transient pulsatile character of the cAMP signal is maintained by extracellular phosphodiesterase to prevent receptor saturation and to reduce the background concentrations of chemokine (52). It takes approximately 2 s for the signal to diffuse between the nearest neighbors (maximal signal range = 72 μm), 2 min for a chemotactic response to occur, and 2–10 min for autonomous signal release. Any 'pulse' that lasts longer than any of these processes will likely dampen the efficiency of chemokine sensing and suppress further cAMP release (53).

Dictyostelium move at 5–8 $\mu m\ min^{-1}$ with a persistence time of 5 min in a given direction and net length of 20 μm before making a turn (53). Instead of tumbling as bacteria do in order to change the direction of travel, cells make small angular deviations by retracting the pseudopod and forming a new leading edge (54, 55). These properties are remarkably similar to the migration of T lymphocytes in the lymph node, but T cells move even more rapidly in the lymph node. The slime mold model of aggregation may have implications for the aggregation of T cells near or within DC areas of the lymph node early in the immune response (56, 57). Even though T cells have not been shown to secrete chemoattractants for each other resulting in the propagative wave and cooperativity of aggregation observed in *Dictyostelium*, the same concern of receptor saturation applies to chemoattractants in the immune system.

Neuronal growth cones

An elegant series of investigations by Mu-ming Poo and colleagues (58) have established cellular pathways involved in chemoattraction and repulsion used in neuronal path finding. Using pipettes to release substances and a quantitative assay of turning behavior, attraction toward the chemokine stromal cell-derived factor-1 (SDF-1) was shown to be mediated by IP_3 generation and the resultant Ca^{2+} signal (58). Repulsion from a γ-aminobutyric acid (GABA)-receptor agonist was mediated by activation of protein kinase C (PKC). Both repulsive and attractive signals are generated by GPCR, but attraction is favored by elevating cGMP or by inhibiting PKC. This investigation demonstrates a hierarchy of signals, initiated by GPCR and integrated within the cell, that can cause growth cone attraction or avoidance. In another study (59), local Ca^{2+} signaling was shown to occur spontaneously in filopodial processes during motility promoted by particular substrates; these signals depended upon Ca^{2+} influx but were not mediated by voltage-gated Ca^{2+} channels. Local clusters of integrin receptors may underlie the Ca^{2+} influx, as suggested by the substrate dependence and confirmed by the ability of a specific arginyl-glycyl-α-aspartyl-serinyl (RGDS) peptide that activates β1 integrin receptors to elicit Ca^{2+} transients and by antibodies to β1 integrins to block them. Like Ca^{2+} puffs and sparks that can summate to produce propagated Ca^{2+} waves, such local Ca^{2+} signals can be summed to produce larger signals that evoke turning behavior at the interface between different substrates. Such a mechanism might very well apply locally at compartmental boundaries in secondary lymphoid tissue.

Leukocytes: neutrophils and macrophages

Motility and chemotaxis in higher eukaryotes have been well characterized in polymorphonuclear neutrophils (PMNs) and macrophages, and they share many similarities with that in *Dictyostelium*, with signal transduction occurring through a

G-protein-linked pathway in all organisms despite evolutionary separation and diverse chemoattractants. Leukocytes undergo amoeboid chemotaxis and are thought to prefer a spatial sensing mechanism, although both sensory modalities could be employed. For a round, stationary amoeboid cell, the initial chemotactic stimulus leading to polarization may be sensed spatially and maintained during chemotaxis by a localized sensitivity to chemoattractant concentrations along cell surface (31). A wide range of substances have been found to stimulate chemotaxis in leukocytes (PMN and macrophages), including f-Met-Leu-Phe (fMLP), leukotriene B_4 (LTB_4), platelet-activating factor (PAF), lysophosphatidic acid (LPA), the cleavage product of complement component 5 (C5a), oxidized lipids, and denatured proteins (37, 60–63). Receptors for N-formylated peptides have been isolated (64) and found to internalize upon ligand binding (49, 65). fMLP receptors in neutrophils localized to the anterior or mid-region of a cell with the fewest receptors at the trailing edge (66), but binding of fMLP to receptor was not necessary for the development of asymmetry in one report (67). C5a and interleukin-8 (IL-8) receptors on human neutrophils are constitutively clustered with no change in distribution upon activation by fMLP (68). It is unclear what role these spatial patterns of receptor localization on the membrane play in gradient sensing, polarity, or chemotaxis. This failure of chemoattractants to stimulate chemoreceptor redistribution in neutrophil and ameba provides support for signal transduction restricted to the leading edge, which leads to local activation of cytoskeleton. Alternatively, a 'lateral pseudopod inhibition' effect may prevent the rest of the unstimulated cell surface from forming pseudopodia (69). In some instances, adhesion through integrin receptors and migration is necessary to induce the polarization of these receptors. In neutrophils, studies of responses between competitive sources of different chemokine gradients in an under-agarose gel assay revealed a curious hierarchy of chemoattractant sensitivity, with the dominant chemokines (fMLP and C5a) being controlled by the p38 mitogen-activated protein kinase (MAPK) signaling pathway, that can additionally suppress the response to 'intermediate' or 'weaker' chemokines (IL-8 and LTB4) that are controlled by a PI3K/Akt pathway (70). These chemokine hierarchies may be relevant in physiological conditions, where overlapping chemokine gradients must ultimately give cells the signal to be allocated for more urgent functions by migrating to the correct tissues.

Methods to investigate chemotaxis

The Boyden chamber

In 1962, Boyden developed a transwell assay (71), which has become a standard procedure for investigating chemotaxis (*Fig.* 8). The magnitude of the chemotactic response can be quantified by counting the number of cells that have traversed the filter in comparison to basal levels of transmigration in the absence of chemokine. As more knowledge is amassed about the physiological context of chemotaxis and chemokine distribution in tissues, this assay has been modified for studying migration on specific extracellular matrix proteins or movement across seeded monolayers to simulate transendothelial migration (as in extravasation).

Transwell assays are convenient for screening and are easy to perform, but they can give misleading information, since the results can be affected by changes in adhesion, motility, or spatial orientation. For example, an increase in motility (chemokinesis) would increase migration of randomly directed cells and might score as chemotaxis in many studies. One basis for distinguishing chemotaxis from chemokinesis is the statistically insignificant increased rate of random migration in a uniform concentration of chemokine. The placement of a chemoattractant into the lower chamber creates a crude gradient across the filter that can be sensed by motile cells placed into the upper chamber. However, chemokines can be severely depleted from the chamber by binding to surfaces (72). Gravity can also bias locomotion of cells in a Boyden chamber (73). Shear forces and the physiological chemokine density on blood vessels play an important role in transmigration, but these conditions cannot be simulated with the classic transwell migration assay. The gradient across barriers of artificial filters or reconstituted endothelial monolayers can induce transwell migration but does not necessarily reflect a physiologically relevant distribution of chemokine. Moreover, this assay cannot be used to determine the speed of cell migration. The optimal length of time to see an effect in the Boyden chamber assay is 1–4 h (74, 75), due to the tendency for cells to travel laterally or become trapped within the filter (76). This timing does not correlate well with *in vivo* kinetics of extravasation, in which rolling, adhesion, and extravasation of leukocytes occurs over the course of minutes (7, 77). A further conundrum concerns the dose–response relationship of cell migration in the Boyden chamber assay and its relation to chemotaxis. Migration toward a chemoattractant diffusing away from a source could occur at distances of up to 250 μm (78). This finding would imply that a cell should be able to detect a gradient at both high concentrations near the source and low concentrations farther away, according to an inverse-square function predicted by diffusion. However, migration in the Boyden chamber exhibits a steep concentration dependence and motility is inhibited above the optimal concentration. Given the potential pitfalls and uncertainties

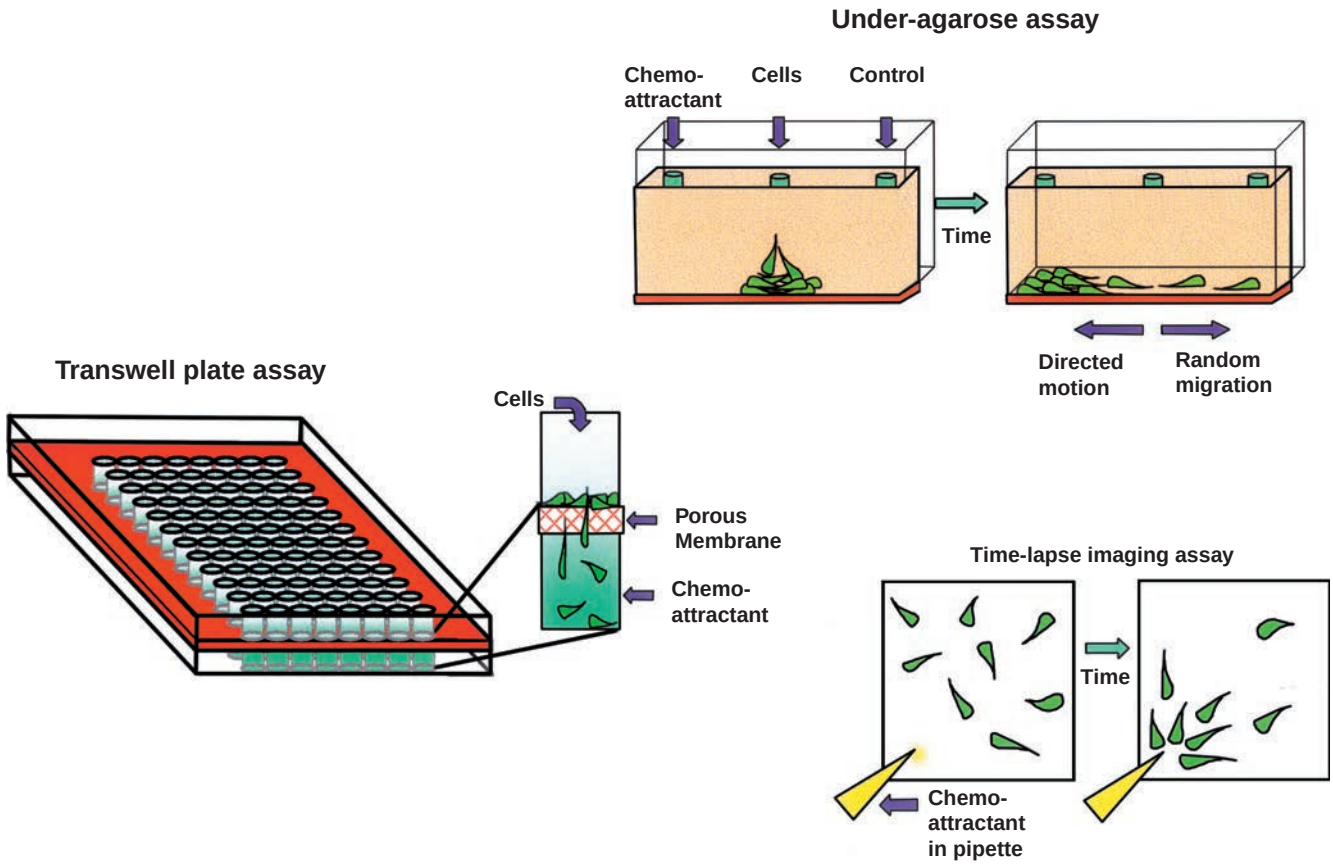

Fig. 8. Methods to investigate chemotaxis.

with the Boyden chamber approach, imaging methods that have been applied successfully to investigate chemotaxis in other cell types seem preferable.

Imaging chemotaxis

A variety of chambers have been developed to visualize the movement of cells within a linear gradient of chemoattractant in liquid culture or solid media or incorporating cells as substrates. The Dunn direct-viewing chemotaxis chamber is built upon the principles of the Zigmond chamber, and it offers the ability to image migration within a linear chemoattractant gradient (79). Heit and Kubes have developed an under-agarose cell migration assay for chemotaxis and chemokinesis that can create an environment of complex combinations of both spatial and temporal chemotactic gradients and can be adapted for real-time imaging and fluorescence studies (*Fig.* 8) (80). Cinamon *et al.* (76) have developed a real-time *in vitro* technique to visualize adhesion and signaling through GPCR during transmigration of lymphocytes. In addition to reconstituting a monolayer of activated endothelial cells stimulated with cytokines to mimic the adhesive ligand expression of inflamed vessels (74, 75) as in some Boyden chamber assays, this method introduced laminar flow to produce physiological levels of shear force that are known to enhance adhesion of leukocytes. Chemokines are loaded onto the surface of endothelial cells and washed. However, this method of chemokine presentation cannot simulate chemokine transport or the sublumenal composition of chemokines that would exist in tissue. Some real-time imaging experiments attempt to create a diffusion gradient (without flow in this instance) by using a point source of chemokine, as from a pipette tip (*Fig.* 8). Such experiments have convincingly demonstrated chemotaxis in *Dictyostelium*, neuronal growth cones, and neutrophils, but the capability of lymphocytes to undergo directed motion in a chemokine gradient has not been well documented.

Lymphocyte chemotaxis *in vitro*

Chemokines mediate several effects on lymphocytes, including a hierarchy of interactions with TCR signaling (81). Repulsive chemokine interactions have been reported for T cells and may have relevance to thymic homing (82, 83). However, imaging studies that directly demonstrate fundamental properties of

lymphocyte chemotaxis are lacking. Part of the reason for this dearth may be that chemotaxis can be context dependent, requiring a particular substrate to 'present' the appropriate bound chemokine. Haptotactic gradients have not yet been investigated thoroughly, although there is at least one indication that these can produce non-uniform distributions of T cells (72). It may be more realistic to investigate haptotaxis rather than chemotaxis, using gradients of chemokines deposited on defined substrates. Finally, to mention an intriguing recent report, the ionotropic glutamate receptor GluR3 has been implicated in lymphocyte adhesion and chemotaxis (84). Physiological concentrations of glutamate-stimulated lymphocyte adhesion to laminin and fibronectin by acting through integrins and enhanced chemotaxis of T cells in response to SDF-1α. Further mechanistic research using imaging approaches is warranted to assess chemotaxis in lymphocytes.

When we envision chemotaxis, videos of *Dictyostelium* moving toward a point source of cAMP or neutrophils chasing bacteria come to mind. Unfortunately, little or no evidence exists showing that lymphocytes are capable of responding by moving toward the source of a chemoattractant. The known chemotaxing or chemotropic cells (*Dictyostelium*, *Saccharomyces cerevisiae*, neutrophils) and neuronal growth cones all use GPCR to detect chemoattractants and utilize signal transduction pathways that are similar for chemokine receptors in the immune system. Membrane ruffling, PI3K activity, and the resulting PIP_3 products are localized at the stimulated edge in a chemokine gradient during exposure to chemokines in neutrophils (85), *Dictyostelium* (86), fibroblasts (87), and occur in T cells during the early stages of contact with APCs (88). From the above, it is evident that lymphocytes exhibit motility properties similar to those in other eukaryotic cells and possess chemokine receptors, but little is known about specific properties of chemotaxis in lymphocytes. Our observation of randomly oriented T cells exhibiting vigorous motility in the lymph node prompts the question of whether chemotaxis plays any role during antigen recognition in the lymph node, perhaps by exerting an undetectable bias upon the seemingly random migration or in local regions that have not been examined thus far.

Polarity of chemokine receptors: evidence for chemotaxis?

As in neutrophils, but not *Dictyostelium* (see above), chemokine receptors can adopt a polarized distribution in lymphocytes. Chemokine receptors CCR2, CCR5, and CXCR4 are located preferentially at the leading edge in the appropriate lymphocyte subsets (72, 89–91), as are links to cytoskeletal elements. However, any substance capable of inducing polarity, including the chemotactic peptides MCP-1 (monocyte chemotactic protein-1), RANTES (regulated upon activation, normal T-cell expressed, and presumably secreted), and IL-8, and the cytokines IL-2 and IL-15, can evoke redistribution of a chemoreceptor specific to a different chemokine (89). Receptor aggregation in an anterior compartment may play a chemotactic role in leading edge formation and perhaps can reduce the availability of receptors for the formation of a new leading edge once the angle of trajectory has been established. In addition, maintenance of directional migration may be limited by the time necessary to rearrange the cytoskeleton to form a new filopodium, thus preferring slight angular changes in areas of shallow chemokine gradient (69). Chemokine signaling is known to influence cytoskeleton rearrangements to initiate polarization and directional migration. Evidence of direct interaction of chemokine receptors to motor proteins was shown by the constitutive association of the C-termini of CXCR4 and CXCR5 chemokine receptors with the motor protein nonmuscle myosin H chain-IIA (NMMHC-IIA) in T lymphocytes (92). It has been previously shown that CXCR4 and myosin light chain (MLC) act together at the leading edge of lymphocytes to shape actin polymerization (89, 93). Confocal imaging has revealed that CXCR4, NMMHC-IIA, F-actin, and MLC are colocalized at the leading edge in SDF-1α-treated lymphocytes adhered to fibronectin, while ICAM-3 and NMMHC-IIB are redistributed to the uropod (92, 94). Studies on *Dictyostelium* mutants lacking myosin heavy chain show a twofold reduction in polarization and migration, and when placed within a cAMP gradient, these mutants exhibit significantly reduced chemotaxic index compared to wildtype (95). Together these studies suggest a role for myosin heavy chain in regulating polarity formation, even though it is not required.

Although studies in lymphocytes provide a first look at mechanosignaling mechanisms of chemotaxis, they do not directly test the contribution of a chemokine gradient in mediating receptor polarization. The inability of chemokine treatment to alter the constitutive nature of CXCR4–NMMHC-IIA association means that colocalization does not merely optimize signaling distance between these two proteins but rather enhances chemoreception at the leading edge to promote adhesion. Although many cell types rely upon GPCR for chemotaxis, there is still no evidence of receptor redistribution along the cell surface being essential for formation of polarity, although there is evidence for non-specific polarity (induced by another chemokine) being a requirement for chemoreceptor redistribution. There is also no evidence

that other mechanisms of localized chemoreceptor modification that may occur after ligand binding, such as phosphorylation of GPCR, plays a role in amplifying the signal. Chemotaxis remains intact in *Dictyostelium* and leukocytes with deletion of phosphorylation sites (96–98).

Polarity of antigen responsiveness

In most *in vitro* studies, as we have observed in the lymph node, the T cell normally initiates contact with an APC by crawling toward the APC. A crawling T cell functions as a polarized antigen sensor by virtue of increased sensitivity to contact at the leading edge. Ca^{2+} signaling is activated preferentially by contact at the leading edge, either with an APC bearing specific antigen or with beads coated with anti-CD3 antibodies as surrogate APC (17, 99). The polarity of antigen detection is very strong, as demonstrated by mapping with beads 3–6 μm in diameter (99). Ca^{2+} signaling was detected in >90% of trials with contact at the leading edge and <10% at the trailing edge. Recently, a similar degree of polarity was obtained using single nanosphere-labeled peptides bound to APCs (100). The molecular basis for polarity is unknown but could involve activation by molecules preferentially found at the leading edge or inhibition, possibly steric in nature, by molecules at the trailing edge of the cell. One candidate inhibitory molecule, CD43, is a bulky glycoprotein preferentially localized at the trailing edge of a migrating T cell, but when CD43 was delocalized by mutation of an ezrin-binding motif, signaling and polarized motility remained intact (18). Regardless of the mechanism for polarized detection of antigen, migrating T cells would be more likely to contact APCs by random collisions at the leading edge merely by virtue of the direction of travel.

Immunological synapse

Once contact has been established, a complex sequence of molecular rearrangements takes place, giving rise to the 'immunological synapse' (101). Receptors, kinases, and cytoskeletal elements segregate into central and peripheral supramolecular activation clusters (c- and p-SMACs) in the zone of contact (102, 103) forming close molecular associations. Several excellent reviews on T-cell signaling and the IS have appeared recently (104–107). Some molecular rearrangements can occur within minutes. Movement of TCR molecules, tracked as an ensemble or as single molecules tagged with fluorescent nanospheres (30 nm in diameter), toward the c-SMAC occurs too rapidly to be explained by a diffusion trapping mechanism and may instead reveal an active mechanism that involves cytoskeletal rearrangement (108). Longer term changes involving costimulatory molecules can evolve over 2–48 h in the IS (107). Confocal microscopy of fixed lymph node tissue has shown that some elements of the IS are present in T cells interacting with DCs *in vivo* (109). However, the stability of the synapse may depend upon the cell culture system or the types of cells employed. In liquid culture systems with cell lines used as APCs or a lipid bilayer containing peptide MHC to 'present' antigen, the IS tends to be stable, while in the collagen gel culture system, interactions of T cells with antigen-bearing DCs were transient and dynamic in nature (110, 111). It is clear that environmental factors can influence the dynamic properties of the IS. Recently, $CD8^+$ T cells were observed making long lasting but dynamic interactions with antigen-primed, *in vitro*-derived DCs (5). There is increasing recognition that several types of IS exist, and these may exhibit a spectrum of dynamic behavior and requirements for T-cell activation (106). These interactions need to be investigated in the native tissue environment.

Ca^{2+} signaling, ion channels, gene expression

Contact with antigen-primed APCs initiates a local signaling cascade at the IS that gives rise to a global Ca^{2+} signal initiated by IP_3-induced release from intracellular stores and sustained by Ca^{2+} influx. The Ca^{2+} signal can be transient, oscillatory, or sustained, depending upon the stimulus intensity and the T-cell subset (17, 104, 112–115). Ca^{2+} influx is required for an extended period for normal T-cell activation. Within the cell, Ca^{2+} signaling modulates the activity of many enzymes, cytoskeletal elements, and ion channels. When oscillatory or sustained, the Ca^{2+} signal leads to gene expression via the calcineurin/nuclear factor for activated T cells (NF-AT) pathway by promoting accumulation of dephosphorylated NF-AT in the nucleus (116). The Ca^{2+}-dependent phosphatase, calcineurin, induces most of the changes in gene expression induced by TCR engagement in human T cells (117). Calcineurin inhibition is the basis for clinically used immunosuppressants, such as cyclosporine A and FK506. Intracellular Ca^{2+} levels must remain elevated or oscillate for >1 h in order to induce significant gene expression via calcineurin (114, 118). However, it is apparent that the T cell can integrate signals during transient interactions with APCs *in vitro* and *in vivo* (111, 119).

Ion channels play a key role in generating and shaping the temporal pattern of the Ca^{2+} signal. Two types of Ca^{2+} channels are found in T cells. A CRAC channel mediates Ca^{2+} influx following antigen activation and sustains the Ca^{2+} influx during the initial phase of activation (120). T cells

from severely immunosuppressed patients have been shown to lack functional CRAC channels, highlighting their importance and that of the Ca^{2+} signal itself for the normal immune response (117, 121). Despite the importance of CRAC channels, many mysteries remain regarding their mechanism of activation following depletion of Ca^{2+} stores. Even the molecular identity of the CRAC channel remains enigmatic. Although several candidates including several members of the transient receptor potential (TRP) gene family have been proposed recently, none of these possess the right set of biophysical characteristics, including high selectivity for Ca^{2+} but very low single-channel conductance (122). Compounding the problem, specific blockers of CRAC channels are sorely lacking. A second type of Ca^{2+} channel has been identified at the molecular level and its mode of activation identified, but ironically no function has been ascribed to its channel activity. TRPM7, a member of the TRP gene family, forms a Ca^{2+}- or Mg^{2+}-permeable channel that is blocked by normal levels of cytoplasmic Mg^{2+} (123–126). A very unusual feature of the channel protein is its functional α-kinase domain near the cytoplasmic C-terminus; a possible link between channel activity and kinase activity remains unresolved. Functional expression of the TRPM7 channel is increased 10-fold during T-cell activation, but the significance of this increase is also uncertain (127).

In contrast, progress on K^+ channels has been swift and is leading toward the identification of therapeutic agents to modulate the immune response. Ca^{2+} influx through CRAC channels is sustained by the counterbalancing efflux of K^+ through either voltage-gated Kv1.3 channels or Ca^{2+}-activated IKCa1 channels, depending upon the T-cell activation state and corresponding expression levels of these two K^+ channels. The genes for both K^+ channels have been identified, potent and selective blockers have been identified, and their regulated pattern of expression has been investigated (128, 129). Expression levels of both K^+ channels increase dramatically and in a sequential manner during progression from a resting T cell to an activated T cell and later to a memory T cell. In particular, IKCa1 levels are upregulated more rapidly [via the PKC pathway and requiring Ikaros and activator protein-1 (AP-1)] than Kv1.3, resulting in T-cell blasts that are dependent upon IKCa1 for continued activation or re-activation (130). If T cells are subjected to multiple rounds of activation to acquire a memory phenotype, Kv1.3 levels gradually increase to the point that they become the dominant K^+ channel in effector memory T cells (131). Changes in the channel expression pattern might allow particular phases of an immune response to be targeted selectively. Chronically activated effector memory T cells that mediate autoimmune reactions may be particularly susceptible to Kv1.3 blockade. In support of this concept, a sea anemone toxin that blocks Kv1.3 selectively was effective *in vivo* in preventing and ameliorating symptoms in adoptive transfer experimental allergic encephalitis (EAE), an animal model for multiple sclerosis (MS) (132). Furthermore, by patch clamp analysis, T cells from patients with MS exhibited very high levels of Kv1.3 channels (133). The development of fluorescent toxin analogs could allow for a simple diagnostic test to detect the upregulation of Kv1.3 in effector memory T cells and to predict the flare-up of an autoimmune reaction (131, 134). K^+ channels in lymphocytes may be linked physically via accessory proteins to lck, CD4, and β integrin molecules as part of a signaling complex and functionally to other vital cell processes including volume regulation, adhesion, and motility (129).

Optimizing the sensitivity of T cells to peptide–MHC

It has been known for some time that low numbers of peptide–MHC complexes (10–100 per cell) on an APC can produce Ca^{2+} signaling and proliferative or effector responses in $CD4^+$ and $CD8^+$ T cells (135–138). Recent work has shown that even a single peptide–MHC complex in the contact zone can evoke a detectable albeit transient Ca^{2+} signal in a T cell (100). This finding of single molecular detection by the T cell has mechanistic implications for signal initiation via the TCR as well as being a wonderful example of intracellular amplification, analogous to the ability of a photoreceptor to detect single photons. Larger numbers of peptide–MHC complexes increased the strength and duration of Ca^{2+} signaling, reaching saturation with only 30–40 molecules of peptide–MHC. Evidence of a stable c-SMAC was found with just 10 molecules of peptide–MHC; recruitment of a vast excess of MHC and TCR molecules to opposite sides of the contact zone evidently does not require continuous ligand–receptor interaction. CD4 plays an important role in increasing the sensitivity, perhaps by dragging the tyrosine kinase lck to the scene, since blocking CD4 shifted the minimally required number of peptide–MHC molecules to >25 (100). Such exquisite sensitivity may involve a series of reversible low affinity interactions between TCR and peptide–MHC within the latency period, since a higher number ($\sim$300) of TCR molecules was required to produce a just-detectable Ca^{2+} signal when relatively high-affinity anti-CD3 antibodies bound to beads were titrated to determine the threshold (99). A further mechanism that may enhance the sensitivity of the T cell is adhesive priming, in which T-cell adhesion, even to glass, can

increase phosphatidylinositol-4,5-bisphosphate (PIP_2) bound to the membrane and the Ca^{2+} content in intracellular stores (139). Coming back to the *in vivo* situation, it is unclear whether non-specific adhesive priming would apply within the lymph node, since T cells already make continuous contact with other cells and reticular fibers before contacting DCs. However, it is clear that the exquisite sensitivity of the immune response requires both molecular mechanisms within the cell to amplify signals and also the scanning process that permits rare T cells to be detected by DC in the lymph node.

Stop signal

In addition to turning on gene expression, the Ca^{2+} signal may affect the formation of the IS and its stability. Contact with APCs initiates dynamic changes in T-cell shape that transiently increases the surface area of contact and helps determine whether T-cell/APC interactions are effective and sustained or abortive. Contact triggers a 'stop' signal that helps anchor a T cell at the site of antigen presentation. The stop signal may originate from the rise in $[Ca^{2+}]_i$. When thapsigargin was used to clamp cytoplasmic Ca^{2+} to varying levels and to bypass normal TCR engagement, elevated $[Ca^{2+}]_i$ by itself was sufficient to inhibit T-cell motility with rapid kinetics via a pathway that does not involve the calcineurin/NF-AT cascade (17). Moreover, when Ca^{2+} was buffered exogenously, the Ca^{2+} signal following contact with APCs was greatly attenuated, and T cells usually made only transient contacts and wandered away from the APCs. In addition, PKC stimulation by itself was also sufficient to immobilize T cells, independent of the rise in $[Ca^{2+}]_i$ (17). During contact with APCs, activation of phospholipase C would lead to both immobilizing signals: Ca^{2+} via IP_3-induced Ca^{2+} release and subsequent activation of the CRAC channel, and PKC activation via diacylglycerol formation. An alternative mechanistic viewpoint was proposed by Dustin and colleagues (140), who invoked integrin interactions in stopping T-cell motility. A recent study provides support for the Ca^{2+} stop signal mechanism (100). Using single-molecule imaging to detect discrete numbers of peptide–MHC complexes in the contact zone, Ca^{2+} flux and a stop signal were tightly linked; both could be triggered by just a single peptide–MHC ligand on the APCs. Higher numbers of peptide–MHC caused more sustained Ca^{2+} signaling and a more robust stop signal. Of course, during normal antigen presentation, the Ca^{2+} signaling, PKC activation, and integrin signaling would all occur and may work synergistically to inhibit T-cell movement away from the site of contact. Departure of a T cell from a DC synapse was associated with a rapid loss of Ca^{2+} signaling (110, 111). Different intensities of Ca^{2+} signaling may provide a graded stop signal, consistent with observations of Ca^{2+} signaling in T cell–DC synapses *in vitro* (111, 135, 141, 142). Contact termination appears to depend upon environmental conditions, as interactions between T cells and DC were either stable in liquid culture (142) or transient in the collagen gel culture system (111).

Antigen-free synapses and crosstalk with DCs

Signals between the T cell and the DC can occur even in the absence of antigen. Ca^{2+} imaging of $CD4^+$ T cell–DC synapses *in vitro* has shown that a DC completely devoid of specific antigen, even lacking MHC, can send a signal to the T cell that is revealed by a Ca^{2+} transient (135, 141, 142). The Ca^{2+} signal in the T cell was more robust and 100% reliable with antigen-bearing DCs, but the fact that it can occur without antigen and is not MHC restricted reveals a novel type of coordination, suggesting the formation of a temporary antigen-free synapse. Antigen-independent signaling also elicited tyrosine phosphorylation, T-cell proliferation, and enhanced long-term survival (141, 142). Transient interactions between T cells and DC under antigen-free conditions in the lymph node likely reflect an interaction that leaves a trace, a memory of contact in the form of a survival signal that may help maintain the naïve T-cell pool *in vivo*. Trautmann's research (142) also revealed another surprising aspect of the T cell–DC interaction. The DC, when it presents antigen, can receive information back from the T cell, as recognized by a Ca^{2+} signal in the DCs (142). The DC Ca^{2+} signal was initiated in approximately 30% of contacts with a lag following initiation of the T-cell signal that occurred reliably during every contact. DCs were also shown to be sensitive to other environmental signals and produced Ca^{2+} signals during adhesion to substrate and exposure to chemokines or to a purinergic P_{2U} agonist but not in response to cross-linking MHC class II molecules. Elevated $[Ca^{2+}]_i$ in the DC, however, did not alter its ability to present antigen to the T cell. These bi-directional signaling interactions hint at additional functions of the IS.

Chemokines and chemotaxis *in vivo*

Chemotaxis or chemotropism is necessary for a variety of crucial functions in higher eukaryotes, including fertilization of an egg by sperm, migration of endothelial cells in angiogenesis, turning of neuronal growth cones in neurogenesis, migration of fibroblasts in wound healing, and thymocyte compartmentalization during embryogenesis. In the immune

system, despite the lack of mechanism-based studies on chemotaxis, a variety of evidence indicate that chemokines and their receptors regulate the migration of leukocytes in response to inflammation and homing of DCs and naïve lymphocytes to their proper lymphoid tissues to facilitate proper cell–cell interaction and tissue homeostasis. In addition, dysregulation of chemotaxis is responsible for the development of numerous pathological conditions from autoimmunity and chronic inflammatory conditions to immunodeficiency and even cancer.

Possible functions for lymphocyte chemotaxis

Chemotaxis has been invoked as a possible mechanism for lymphocyte homing to specific tissue locations, for maintaining compartmental boundaries in secondary lymphoid tissue, and for recruitment of T cells to APCs. By evoking Ca^{2+} signals and other signaling pathways, chemokines may influence many cellular processes in addition to the possibility that they mediate chemotaxis. For chemotaxis to work, there would need to be spatially defined gradients in the right places and cells with the right set of receptors to sense and respond to these with directional motility. *In vivo* studies that have been interpreted as evidence for chemotaxis are reviewed below, along with alternative interpretations.

Chemokines as tissue-specific homing signals

Tissue-specific B- and T-lymphocyte adhesion and homing

For many years, *in vivo* studies have demonstrated the importance of chemokines as tissue-selective homing factors, especially in the process of extravasation of leukocytes across endothelial barriers. A combination of shear force and high chemokine receptor occupancy may be crucial for mediating homing in leukocytes (143). B and T lymphocytes undergo tethering and rolling upon the surface of high endothelial venule (HEV) through the interaction of L-selectin and peripheral node addressin (PNAd). When chemokines initiate signaling through a $G_{\alpha i}$-coupled receptor, lymphocyte adhesion is triggered by an increased affinity of leukocyte function-associated antigen-1 (LFA-1) for ICAM-1 (144–147). The nature of this adhesion is selective for T-cell subsets. Whereas macrophage inflammatory protein-3α [MIP-3α] can induce adhesion in some subsets of $CD4^+$ memory T cells, the chemokines SDF-1α, a secondary lymphoid chemokine (SLC), and EBI-1-ligand chemokine (ELC/MIP-3β) can effect adhesion in most peripheral blood lymphocytes including naïve T cells (143, 146). Adhesion for other memory T-cell subsets is mediated by the ligands for CXCR3 [interferon-inducible protein-10 (IP-10) or monokine induced by γ-interferon (Mig)], CCR4 [macrophage-derived chemoattractant (MDC), or thymus and activation-regulated chemokine (TARC)], or CCR1 and CCR5 (RANTES) (148–150). The first homing chemokine for lymphoid tissue, SLC, enhanced β2 integrin-dependent adhesion of naïve T cells under flow (151). This chemokine is expressed on the HEV of lymph node and Peyer's patches, on lymphatic endothelium of many organs, and within T-cell areas of the spleen, lymph nodes, and Peyer's patches (151–153). Mutant *plt* (paucity of lymph node T cell) mice are deficient in ELC and lymphoid-expressed SLC (154–156). These mice exhibit deficits in T-lymphocyte homing at the adhesion step, but this defect can be reconstituted by subcutaneous injection of SLC due to transport of SLC to draining lymph nodes, where they are subsequently transported to the surface of endothelial cells (153). ELC or MIP3β, another ligand for CCR7, is expressed in the T-cell areas of lymph node but not in quantities great enough to rescue lymphocyte adhesion in the HEV of *plt* mice (154). B-cell homing and adhesion to HEV were reduced twofold in lymph nodes of *plt* mice; in contrast, homing to Peyer's patches was barely affected (157). These studies suggest that B-cell homing in lymph nodes is highly sensitive to the loss of CXCR4 and CCR7, while Peyer's patches require the additional loss of CXCR5 (157). It should be noted, however, that the relatively unaffected homing of wildtype B cells into *plt* mice compared to the reduced homing of $CCR7^{-/-}$ B cells in wildtype mice may be attributed to a small amount of non-lymphoid-expressed SLC present on the HEV (157). The diverse requirements for homing of B and T lymphocytes suggest that chemokines may undergo different mechanisms of transport through tissue (158) and may mediate disparate functions, even though they may share a common receptor.

Selective B-cell homing is mediated by B-lymphocyte chemoattractant [BLC/CXCL13/B cell-attracting chemokine-1 (BCA-1)] that binds CXC chemokine receptor 5 (CXCR5) and is expressed in the follicles of lymph nodes, spleen, and Peyer's patches (159). BLC is crucial for the development of lymphoid tissues, while both ligand and receptor are necessary for homing of B cells to lymph node and spleen (160). The role of B-cell-specific chemokines in homing is reviewed by Cyster and colleagues (161).

The process of endothelial adhesion requires a much higher number of occupied chemoreceptors than needed to stimulate chemotaxis, thus raising questions about the differences between physiological chemokine concentrations presented

on vascular endothelium and within tissue (149). In order for the homing process to be considered transendothelial chemotaxis, there must a diffusible chemokine gradient at the endothelial–flow interface, or a soluble or haptotactic gradient across the endothelial barrier. The equilibrium between chemokine transport to HEV and chemokine production within tissue will be a major consideration in the maintenance of any gradient. Evidence for and against these putative gradients will be discussed later.

Evidence that chemokines allow direct homing into lymphoid compartments, rather than necessitating migration through tissue

It has been shown that T cells adhere only to specific areas of the HEV where SLC is expressed. B cells do not home to the same region of the HEV in Peyer's patches, but they adhere to regions upstream to the site of T-cell adhesion that are more proximal to follicles (152). This separation implies a plausible mechanism for compartmentalization based upon sorting of naïve T and B cells at homing sites, rather than depending upon complex gradients of T- and B-cell chemokine to direct chemotactic sorting within the cortex (Fig. 9). However, the role of chemokines and chemoreceptors may vary according to the cell type. CCR7-deficient mice demonstrate impaired homing to lymph node and Peyer's patch of both B cells and T cells (162), in agreement with *in vitro* data showing chemotactic response of B cells to ELC and SLC as well as expression of CCR7 on the B-cell membrane (146, 151, 163–165). Thus, homing and function of B cells require not only the association of CXCR5 and BLC but also the CCR7 receptor. In addition, mature DCs are no longer able to migrate to draining lymph nodes in CCR7-deficient mice (162). SLC-deficient *plt* mice also exhibit a threefold reduction in the number of DCs that are able to home to the T-cell areas of lymph node and spleen (166). It is no surprise that the complexity of the immune system demands fine control of immune cell responses to environmental or inflammatory cues, giving rise to the idea of combinatorial control in lymphocyte chemotaxis (167). Lymphocytes must be able to integrate competing or conflicting chemoattractive sources in a complex setting, especially as they undergo various stages of differentiation and maturation, in order to respond properly within the context of this signal. This leaves open the question of whether these complex chemokine signals exist as soluble gradients, haptotactic sources, uniform concentrations, or transient pulsatile releases on endothelium or within tissue.

Nature of chemokine distribution and presentation

Evidence for soluble and immobilized chemokines

Immobilized chemokines may play a role under conditions that cannot support maintenance of a soluble chemokine gradient. The flow of blood within the lumen of vessels is likely to dissipate any soluble chemokines secreted from the apical side of endothelial cells, suggesting that adhesion under flow is mediated predominantly by haptotactic presentation of chemokines, as demonstrated by the ability of membrane-bound Groα to induce monocyte adhesion, whereas MCP-1 is ineffective unless added to the perfusion solution (168–170). In the absence of a soluble luminal gradient under shear flow, adhesion and diapedesis of cells across the endothelium may not qualify as a true chemotactic process unless the maintenance of a gradient across the endothelial barrier can be shown. There is evidence that transendothelial migration can occur in the absence of a gradient, as long as

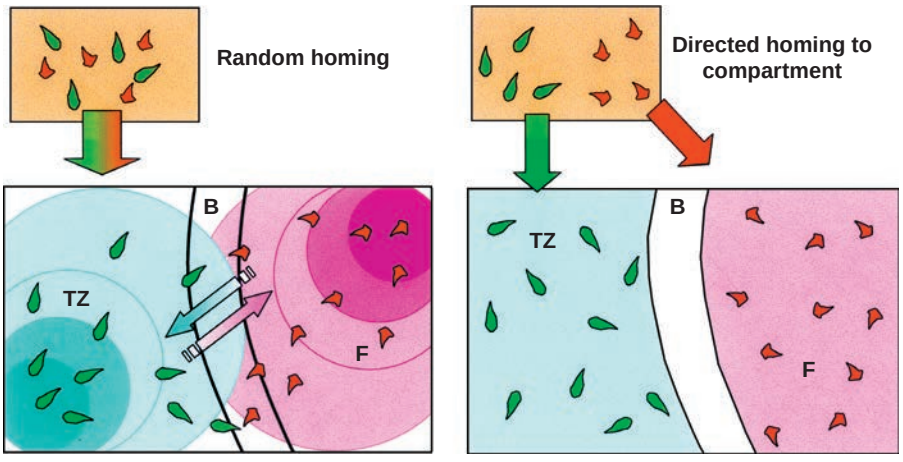

Fig. 9. Alternative models for lymphocyte compartmentalization.

there exists a high concentration of chemokines immobilized on the luminal surface as well as continuous physiological shear stress on migrating lymphocytes (171). Fluid shear has been proposed to modulate G_i protein-mediated chemokine signaling via mechanical mechanisms. Many experiments demonstrating transendothelial chemotaxis are performed with soluble chemokine added to the perfusate, or in the absence of flow. Chemokines can stimulate homing in these cases, but their presentation does not reflect physiological conditions in tissue. As chemokine is also secreted by stromal cells and APCs within lymphoid tissues, is it possible that they can form gradients there?

Physiological chemokine transport

Under inflammatory conditions, it has been shown that soluble chemokines and other low molecular weight factors, produced or deposited subcutaneously in the peripheral tissue, can be carried by draining lymph into lymph nodes through the subcapsular sinuses, then are conducted by the reticular fiber network to the basolateral and apical surfaces of endothelial cells (172, 173). These transported chemokines include IL-8, SLC and ELC for T-cell homing and MCP-1 for monocyte recruitment. In the case of MCP-1, the predominant source of chemokine on the surface of HEV comprises chemokine transported from the skin rather than that being made within lymph node (172). Even in the presence of significant lymph node distortion, the soluble factors are not permitted to diffuse through the lymphoid compartments except when associated with reticular fibers. Additionally, soluble cytokines have been observed to be transcytosed from the abluminal side of endothelial cells to be presented on the lumen of HEV (174). Again, this body of evidence suggests that chemokines involved in homing events act mainly as factors presented on the surface of endothelium, rather than as a soluble gradient, and may not always be derived from lymphoid tissue. The cellular microenvironment of the cortex also seems to be impervious to contribution from peripheral chemokines. To date the spatial distribution of putative chemokine gradients (not merely chemokine expression) have not been visualized, neither the large-scale chemokine gradients thought to direct lymphocyte trafficking nor the small-scale gradients thought to optimize T cell–APC interactions.

Summary and qualifications

A body of literature summarized above suggests that chemokine gradients could be the basis for the cellular compartmentalization of secondary lymphoid organs. However, most of the evidence is indirect. These studies include work with mutant and knockout mice that show disorganized secondary lymphoid structure associated with particular chemokine and receptor deficits. Furthermore, results from *in situ* hybridization on lymph nodes and Peyer's patch show compartment-specific expression of B-cell chemokines in follicles and T-cell specific chemokines in the T zone. However, it is unclear whether the chemokines required for the organization of secondary lymphoid tissues define compartmental boundaries by actually forming gradients, as T-cell chemotaxis in these regions has never been directly observed. Sorting of cells by allowing selective entry into lymphoid compartments according to recognition signals on HEV might provide an alternative mechanism for separation of T and B cells into different compartments (*Fig.* 9). These issues await clarification, with potential contributions from detailed observation and analysis of time-lapse two-photon images.

Thus far, there has been no immunohistochemical evidence for a graded deposition of chemokines in lymphoid tissue compartments. The existence of rapidly motile cells within the densely populated tissue environment of a lymph node makes soluble chemokine gradients unlikely. Solid phase (haptotactic) gradients may promote chemotaxis in particular locations, but these have not been seen. Immunohistochemistry and *in situ* hybridization have been utilized to probe for chemokine expression. However, to reveal gradients of chemokines within tissues, different approaches might be required. Moreover, is the chemokine delivered as a uniform concentration, a shallow gradient, or a steep gradient? To what extent is the chemoattractant further regulated by extracellular degradation, as for neutrophils and *Dictyostelium* (175–177)? The complexity of secretion, diffusion, and regulation of multiple chemokines within a highly cellular lymphoid environment cannot be simulated by *in vitro* studies, nor can its effects be dynamically visualized in histological sections. Both neutrophils and *Dictyostelium* exhibit a wide range of responses to uniform chemokine concentrations, including increased adhesion, further secretion of chemotactic substances, pinocytosis, and chemokinesis. In the absence of conclusive evidence for the presence of a chemokine gradient within tissue, it is possible that lymphokines primarily serve different biological functions than to direct cellular trafficking through lymphoid organs, or to promote cell–cell contact during antigen presentation.

Future directions and challenges for *in vivo* imaging

In this review, we have highlighted results using two-photon imaging techniques and compared what we have observed

thus far with a much larger literature that describes *in vitro* experiments on motility, chemotaxis, and antigen responses. In addition, we discuss a portion of the huge literature on effects of chemokines *in vivo* and raise the question of whether chemokines mediate homing and compartmentalization via chemotaxis or other possible mechanisms. Broadly speaking, the potential is great for two-photon imaging to shed light on mechanisms that we have touched upon in this survey of the literature. Given the differences seen thus far between the stability of IS under different conditions, it will be exciting to visualize and compare cellular dynamics in the diversity of IS. A wide variety of transgenic models are available to visualize different cell types and to probe specific molecular requirements for rapid motility and responses to antigen. Methods to image $[Ca^{2+}]_i$ and gene expression quantitatively in the living tissue will be needed to resolve some of these issues. The feasibility of imaging in lymph node and spleen has already been demonstrated; the method should also be readily adaptable to peripheral tissues and to models for tumor formation and immunotherapy. It should be possible to adapt explanted lymphoid organs and two-photon imaging to test candidate immunosuppressive molecules in a realistic setting.

Supplementary material

The following material is available from http://www.blackwellpublishing.com/products/journals/suppmat/imr/imr076/imr076sm.htm. Typical lymphocyte motility patterns near a primary follicle in murine lymph node as observed by two-photon microscopy. Time-lapse images of T cells (green) and B cells (red) from normal mice move along random paths in the T zone and follicle, respectively. Each frame represents an imaging volume approximately 220 × 180 × 75 m. Time is indicated in the lower left corner of each frame.

References

1. Cahalan MD, Parker I, Wei SH, Miller MJ. Two-photon tissue imaging: seeing the immune system in a fresh light. Nat Rev Immunol 2002;**2**:872–880.
2. Miller MJ, Wei SH, Parker I, Cahalan MD. Two-photon imaging of lymphocyte motility and antigen response in intact lymph node. Science 2002;**296**:1869–1873.
3. Stoll S, Delon J, Brotz TM, Germain RN. Dynamic imaging of T cell–dendritic cell interactions in lymph nodes. Science 2002;**296**:1873–1876.
4. Wei SH, Miller MJ, Cahalan MD, Parker I. Two-photon imaging in intact lymphoid tissue. Adv Exp Med Biol 2002;**512**:203–208.
5. Bousso P, Robey E. Dynamics of $CD8^+$ T cell priming by dendritic cells in intact lymph nodes. Nat Immunol 2003;**4**:579–585.
6. Bousso P, Bhakta NR, Lewis RS, Robey E. Dynamics of thymocyte–stromal cell interactions visualized by two-photon microscopy. Science 2002;**296**:1876–1880.
7. Miller MJ, Wei SH, Cahalan MD, Parker I. Autonomous T cell trafficking examined in vivo with intravital two-photon microscopy. Proc Natl Acad Sci USA 2003;**100**: 2604–2609.
8. Pawley JB. Handbook of Biological Confocal Microscopy, 2nd edn. New York: Plenum Press 1995.
9. Denk W, Strickler JH, Webb WW. Two photon laser scanning fluorescence microscopy. Science 1990;**148**:73–76.
10. Hopt A, Neher E. Highly nonlinear photodamage in two-photon fluorescence microscopy. Biophys J 2001;**80**:2029–2036.
11. Booth MJ, Neil MA, Juskaitis R, Wilson T. Adaptive aberration correction in a confocal microscope. Proc Natl Acad Sci USA 2002;**99**:5788–5792.
12. Von Andrian UH. Immunology. T cell activation in six dimensions. Science 2002;**296**:1815–1817.
13. Caldwell CC, et al. Differential regulation of physiologically relevant hypoxic conditions on T lymphocyte development and effector functions. J Immunol 2001;**167**:6140–6149.
14. Blaheta RA, et al. In vitro analysis of verapamil-induced immunosuppression: potent inhibition of T cell motility and lymphocytic transmigration through allogeneic endothelial cells. Transplantation 2000;**69**:588–597.
15. Shutt DC, Stapleton JT, Kennedy RC, Soll DR. HIV-induced syncytia in peripheral blood cell cultures crawl by extending giant pseudopods. Cell Immunol 1995;**166**: 261–274.
16. Sylwester A, et al. T cells and HIV-induced T cell syncytia exhibit the same motility cycle. J Leukoc Biol 1995;**57**:643–650.
17. Negulescu PA, Krasieva TB, Khan A, Kerschbaum HH, Cahalan MD. Polarity of T cell shape, motility, and sensitivity to antigen. Immunity 1996;**4**:421–430.
18. Savage ND, Kimzey SL, Bromley SK, Johnson KG, Dustin ML, Green JM. Polar redistribution of the sialoglycoprotein CD43: implications for T cell function. J Immunol 2002;**168**:3740–3746.
19. Niggemann B, Maaser K, Lu H, Kroczek R, Zanker KS, Friedl P. Locomotory phenotypes of human tumor cell lines and T lymphocytes in a three-dimensional collagen lattice. Cancer Lett 1997;**118**:173–180.
20. Fuller CL, Braciale VL, Samelson LE. All roads lead to actin: the intimate relationship between TCR signaling and the cytoskeleton. Immunol Rev 2003;**191**:220–236.
21. Penninger JM, Crabtree GR. The actin cytoskeleton and lymphocyte activation. Cell 1999;**96**:9–12.
22. Rossi D, Zlotnik A. The biology of chemokines and their receptors. Annu Rev Immunol 2000;**18**:217–242.
23. Proudfoot AE, Power CA, Rommel C, Wells TN. Strategies for chemokine antagonists as therapeutics. Semin Immunol 2003;**15**: 57–65.
24. Murphy PM. The molecular biology of leukocyte chemoattractant receptors. Annu Rev Immunol 1994;**12**:593–633.
25. Klinker JF, Wenzel-Seifert K, Seifert R. G-protein-coupled receptors in HL-60 human leukemia cells. Gen Pharmacol 1996;**27**: 33–54.
26. Lad PM, Olson CV, Smiley PA. Association of the N-formyl-Met-Leu-Phe receptor in human neutrophils with a GTP-binding protein sensitive to pertussis toxin. Proc Natl Acad Sci USA 1985;**82**:869–873.
27. Hall AL, Warren V, Condeelis J. Transduction of the chemotactic signal to the actin cytoskeleton of *Dictyostelium discoideum*. Dev Biol 1989;**136**:517–525.
28. Spangrude GJ, Sacchi F, Hill HR, Van Epps DE, Daynes RA. Inhibition of lymphocyte and neutrophil chemotaxis by pertussis toxin. J Immunol 1985;**135**:4135–4143.

29. Tranquillo RT, Lauffenburger DA, Zigmond SH. A stochastic model for leukocyte random motility and chemotaxis based on receptor binding fluctuations. J Cell Biol 1988;**106**:303–309.
30. Mato JM, Losada A, Nanjundiah V, Konijn TM. Signal input for a chemotactic response in the cellular slime mold *Dictyostelium discoideum*. Proc Natl Acad Sci USA 1975;**72**:4991–4993.
31. Devreotes P, Janetopoulos C. Eukaryotic chemotaxis. Distinctions between directional sensing and polarization. J Biol Chem 2003;**278**:20445–20448.
32. Arkowitz RA. Responding to attraction: chemotaxis and chemotropism in Dictyostelium and yeast. Trends Cell Biol 1999;**9**:20–27.
33. Kimmel AR, Parent CA. The signal to move: *D. discoideum* go orienteering. Science 2003;**300**:1525–1527.
34. McRobbie SJ. Chemotaxis and cell motility in the cellular slime molds. Crit Rev Microbiol 1986;**13**:335–375.
35. Parent CA, Devreotes PN. Molecular genetics of signal transduction in Dictyostelium. Annu Rev Biochem 1996;**65**:411–440.
36. Condeelis J, Jones J, Segall JE. Chemotaxis of metastatic tumor cells: clues to mechanisms from the *Dictyostelium paradigm*. Cancer Metastasis Rev 1992;**11**:55–68.
37. Devreotes PN, Zigmond SH. Chemotaxis in eukaryotic cells: a focus on leukocytes and Dictyostelium. Annu Rev Cell Biol 1988;**4**:649–686.
38. Maghazachi AA. Intracellular signaling events at the leading edge of migrating cells. Int J Biochem Cell Biol 2000;**32**:931–943.
39. Lilly PJ, Devreotes PN. Identification of CRAC, a cytosolic regulator required for guanine nucleotide stimulation of adenylyl cyclase in Dictyostelium. J Biol Chem 1994;**269**:14123–14129.
40. Chen MY, Insall RH, Devreotes PN. Signaling through chemoattractant receptors in Dictyostelium. Trends Genet 1996;**12**:52–57.
41. Xiao Z, Zhang N, Murphy DB, Devreotes PN. Dynamic distribution of chemoattractant receptors in living cells during chemotaxis and persistent stimulation. J Cell Biol 1997;**139**:365–374.
42. Kay RR. Chemotaxis and cell differentiation in Dictyostelium. Curr Opin Microbiol 2002;**5**:575–579.
43. Insall R, et al. CRAC, a cytosolic protein containing a pleckstrin homology domain, is required for receptor and G protein-mediated activation of adenylyl cyclase in Dictyostelium. J Cell Biol 1994;**126**: 1537–1545.
44. Lilly PJ, Devreotes PN. Chemoattractant and GTP gamma S-mediated stimulation of adenylyl cyclase in Dictyostelium requires translocation of CRAC to membranes. J Cell Biol 1995;**129**:1659–1665.
45. Ueda M, Sako Y, Tanaka T, Devreotes P, Yanagida T. Single-molecule analysis of chemotactic signaling in Dictyostelium cells. Science 2001;**294**:864–867.
46. Vicker MG, Schill W, Drescher K. Chemoattraction and chemotaxis in *Dictyostelium discoideum*: myxamoeba cannot read spatial gradients of cyclic adenosine monophosphate. J Cell Biol 1984;**98**: 2204–2214.
47. Vicker MG. The regulation of chemotaxis and chemokinesis in *Dictyostelium amoebae* by temporal signals and spatial gradients of cyclic AMP. J Cell Sci 1994;**107**:659–667.
48. Klein C, Juliani MH. cAMP, induced changes in cAMP-binding sites on D; discoideum amebae. Cell 1977;**10**:329–335.
49. Sullivan SJ, Zigmond SH. Chemotactic peptide receptor modulation in polymorphonuclear leukocytes. J Cell Biol 1980;**85**:703–711.
50. Vitkauskas G, Showell HJ, Becker EL. Specific binding of synthetic chemotactic peptides to rabbit peritoneal neutrophils: effects on dissociability of bound peptide, receptor activity and subsequent biologic responsiveness (deactivation). Mol Immunol 1980;**17**:171–180.
51. Chenoweth DE, Lane TA, Rowe JG, Hugli TE. Quantitative comparisons of neutrophil chemotaxis in four animal species. Clin Immunol Immunopathol 1980;**15**:525–535.
52. Konijn TM. Cyclic AMP as a first messenger. Adv Cyclic Nucleotide Res 1972;**1**:17–31.
53. Robertson AD, Grutsch JF. Aggregation in *Dictyostelium discoideum*. Cell 1981;**24**:603–611.
54. Gerisch G. Chemotaxis in Dictyostelium. Annu Rev Physiol 1982;**44**:535–552.
55. Potel MJ, Mackay SA. Preaggregative cell motion in Dictyostelium. J Cell Sci 1979;**36**:281–309.
56. Ingulli E, Ulman DR, Lucido MM, Jenkins MK. In situ analysis reveals physical interactions between $CD11b^+$ dendritic cells and antigen-specific CD4 T cells after subcutaneous injection of antigen. J Immunol 2002;**169**:2247–2252.
57. Ingulli E, Mondino A, Khoruts A, Jenkins MK. In vivo detection of dendritic cell antigen presentation to $CD4^+$ T cells. J Exp Med 1997;**185**:2133–2141.
58. Xiang Y, et al. Nerve growth cone guidance mediated by G protein-coupled receptors. Nat Neurosci 2002;**5**:843–848.
59. Gomez TM, Robles E, Poo M, Spitzer NC. Filopodial calcium transients promote substrate-dependent growth cone turning. Science 2001;**291**:1983–1987.
60. Niedel JE, Cuatrecasas P. Formyl peptide chemotactic receptors of leukocytes and macrophages. Curr Top Cell Regul 1980;**17**:137–170.
61. Schiffmann E, Corcoran BA, Wahl SM. N-formylmethionyl peptides as chemoattractants for leucocytes. Proc Natl Acad Sci USA 1975;**72**:1059–1062.
62. Zigmond SH. Chemotaxis by polymorphonuclear leukocytes. J Cell Biol 1978;**77**:269–287.
63. Chettibi S, Lawrence AJ, Stevenson RD, Young JD. Effect of lysophosphatidic acid on motility, polarisation and metabolic burst of human neutrophils. FEMS Immunol Med Microbiol 1994;**8**:271–281.
64. Niedel J, Wilkinson S, Cuatrecasas P. Receptor-mediated uptake and degradation of 125I-chemotactic peptide by human neutrophils. J Biol Chem 1979;**254**: 10700–10706.
65. Niedel JE, Kahane I, Cuatrecasas P. Receptor-mediated internalization of fluorescent chemotactic peptide by human neutrophils. Science 1979;**205**:1412–1414.
66. McKay DA, Kusel JR, Wilkinson PC. Studies of chemotactic factor-induced polarity in human neutrophils. Lipid mobility, receptor distribution and the time-sequence of polarization. J Cell Sci 1991;**100**: 473–479.
67. Sullivan SJ, Daukas G, Zigmond SH. Asymmetric distribution of the chemotactic peptide receptor on polymorphonuclear leukocytes. J Cell Biol 1984;**99**:1461–1467.
68. Gray GD, et al. Receptors for the chemoattractants C5a and IL-8 are clustered on the surface of human neutrophils. J Histochem Cytochem 1997;**45**: 1461–1467.
69. Firtel RA, Chung CY. The molecular genetics of chemotaxis: sensing and responding to chemoattractant gradients. Bioessays 2000;**22**:603–615.
70. Heit B, Tavener S, Raharjo E, Kubes P. An intracellular signaling hierarchy determines direction of migration in opposing chemotactic gradients. J Cell Biol 2002;**159**:91–102.
71. Boyden S. The chemotactic effect of mixtures of antibody and antigen on polymorphonuclear leukocytes. J Exp Med 1962;**115**:453–466.
72. Pelletier AJ, et al. Presentation of chemokine SDF-1 alpha by fibronectin mediates directed migration of T cells. Blood 2000;**96**: 2682–2690.
73. Braide M, Ebrahimzadeh PR, Strid KG, Bjursten LM. Migration of human granulocytes in filters: effects of gravity and movable gradients of f-MLP. Biorheology 1994;**31**:617–630.
74. Ding Z, Xiong K, Issekutz TB. Regulation of chemokine-induced transendothelial migration of T lymphocytes by endothelial activation: differential effects on naive and memory T cells. J Leukoc Biol 2000;**67**: 825–833.

75. Roth SJ, Carr MW, Rose SS, Springer TA. Characterization of transendothelial chemotaxis of T lymphocytes. J Immunol Methods 1995;**188**:97–116.
76. Cinamon G, Alon R. A real time in vitro assay for studying leukocyte transendothelial migration under physiological flow conditions. J Immunol Methods 2003;**273**:53–62.
77. Von Andrian UH, et al. L-selectin function is required for beta 2-integrin-mediated neutrophil adhesion at physiological shear rates in vivo. Am J Physiol 1992;**263**:H1034–H1044.
78. Francis K, Palsson BO. Effective intercellular communication distances are determined by the relative time constants for cyto/chemokine secretion and diffusion. Proc Natl Acad Sci USA 1997;**94**:12258–12262.
79. Zicha D, Dunn GA, Brown AF. A new direct-viewing chemotaxis chamber. J Cell Sci 1991;**99**:769–775.
80. Heit B, Kubes P. Measuring chemotaxis and chemokinesis: the under-agarose cell migration assay. Sci STKE 2003;**2003**:PL5.
81. Bromley SK, Peterson DA, Gunn MD, Dustin ML. Cutting edge: hierarchy of chemokine receptor and TCR signals regulating T cell migration and proliferation. J Immunol 2000;**165**:15–19.
82. Poznansky MC, Olszak IT, Foxall R, Evans RH, Luster AD, Scadden DT. Active movement of T cells away from a chemokine. Nat Med 2000;**6**:543–548.
83. Poznansky MC, et al. Thymocyte emigration is mediated by active movement away from stroma-derived factors. J Clin Invest 2002;**109**:1101–1110.
84. Ganor Y, Besser M, Ben-Zakay N, Unger T, Levite M. Human T cells express a functional ionotropic glutamate receptor GluR3, and glutamate by itself triggers integrin-mediated adhesion to laminin and fibronectin and chemotactic migration. J Immunol 2003;**170**:4362–4372.
85. Servant G, Weiner OD, Herzmark P, Balla T, Sedat JW, Bourne HR. Polarization of chemoattractant receptor signaling during neutrophil chemotaxis. Science 2000;**287**:1037–1040.
86. Meili R, Ellsworth C, Lee S, Reddy TB, Ma H, Firtel RA. Chemoattractant-mediated transient activation and membrane localization of Akt/PKB is required for efficient chemotaxis to cAMP in Dictyostelium. EMBO J 1999;**18**:2092–2105.
87. Haugh JM, Codazzi F, Teruel M, Meyer T. Spatial sensing in fibroblasts mediated by 3′ phosphoinositides. J Cell Biol 2000;**151**:1269–1280.
88. Harriague J, Bismuth G. Imaging antigen-induced PI3K activation in T cells. Nat Immunol 2002;**3**:1090–1096.
89. Nieto M, Frade JM, Sancho D, Mellado M, Martinez AC, Sanchez-Madrid F. Polarization of chemokine receptors to the leading edge during lymphocyte chemotaxis. J Exp Med 1997;**186**:153–158.
90. Singer II, et al. CCR5, CXCR4, and CD4 are clustered and closely apposed on microvilli of human macrophages and T cells. J Virol 2001;**75**:3779–3790.
91. Vicente-Manzanares M, et al. The chemokine SDF-1alpha triggers a chemotactic response and induces cell polarization in human B lymphocytes. Eur J Immunol 1998;**28**:2197–2207.
92. Rey M, et al. Cutting edge: association of the motor protein nonmuscle myosin heavy chain-IIA with the C terminus of the chemokine receptor CXCR4 in T lymphocytes. J Immunol 2002;**169**:5410–5414.
93. Vicente-Manzanares M, et al. A role for the Rho-p160 Rho coiled-coil kinase axis in the chemokine stromal cell-derived factor-1 alpha-induced lymphocyte actomyosin and microtubular organization and chemotaxis. J Immunol 2002;**168**:400–410.
94. Campanero MR, Sanchez-Mateos P, del Pozo MA, Sanchez-Madrid F. ICAM-3 regulates lymphocyte morphology and integrin-mediated T cell interaction with endothelial cell and extracellular matrix ligands. J Cell Biol 1994;**127**:867–878.
95. Wessels D, Soll DR, Knecht D, Loomis WF, De Lozanne A, Spudich J. Cell motility and chemotaxis in *Dictyostelium amebae* lacking myosin heavy chain. Dev Biol 1988;**128**:164–177.
96. Kim JY, et al. Phosphorylation of chemoattractant receptors is not essential for chemotaxis or termination of G-protein-mediated responses. J Biol Chem 1997;**272**:27313–27318.
97. Hsu MH, Chiang SC, Ye RD, Prossnitz ER. Phosphorylation of the N-formyl peptide receptor is required for receptor internalization but not chemotaxis. J Biol Chem 1997;**272**:29426–29429.
98. Rubin H, Ravid S. Polarization of myosin II heavy chain-protein kinase C in chemotaxing dictyostelium cells. J Biol Chem 2002;**277**:36005–36008.
99. Wei X, Tromberg BJ, Cahalan MD. Mapping the sensitivity of T cells with an optical trap: polarity and minimal number of receptors for Ca(2+) signaling. Proc Natl Acad Sci USA 1999;**96**:8471–8476.
100. Irvine DJ, Purbhoo MA, Krogsgaard M, Davis MM. Direct observation of ligand recognition by T cells. Nature 2002;**419**:845–849.
101. Grakoui A, et al. The immunological synapse: a molecular machine controlling T cell activation. Science 1999;**285**:221–227.
102. Monks CR, Freiberg BA, Kupfer H, Sciaky N, Kupfer A. Three-dimensional segregation of supramolecular activation clusters in T cells. Nature 1998;**395**:82–86.
103. Freiberg BA, et al. Staging and resetting T cell activation in SMACs. Nat Immun 2002;**3**:911–917.
104. Krummel MF, Davis MM. Dynamics of the immunological synapse: finding, establishing and solidifying a connection. Curr Opin Immunol 2002;**14**:66–74.
105. Bromley SK, et al. The immunological synapse. Annu Rev Immunol 2001;**19**:375–396.
106. Trautmann A, Valitutti S. The diversity of immunological synapses. Curr Opin Immunol 2003;**15**:249–254.
107. Tseng SY, Dustin ML. T-cell activation: a multidimensional signaling network. Curr Opin Cell Biol 2002;**14**:575–580.
108. Moss WC, Irvine DJ, Davis MM, Krummel MF. Quantifying signaling-induced reorientation of T cell receptors during immunological synapse formation. Proc Natl Acad Sci USA 2002;**99**:15024–15029.
109. Reichert P, Reinhardt RL, Ingulli E, Jenkins MK. Cutting edge: in vivo identification of TCR redistribution and polarized IL-2 production by naive CD4 T cells. J Immunol 2001;**166**:4278–4281.
110. Friedl P, Gunzer M. Interaction of T cells with APCs: the serial encounter model. Trends Immunol 2001;**22**:187–191.
111. Gunzer M, et al. Antigen presentation in extracellular matrix: interactions of T cells with dendritic cells are dynamic, short lived, and sequential. Immunity 2000;**13**:323–332.
112. Donnadieu E, Cefai D, Tan YP, Paresys G, Bismuth G, Trautmann A. Imaging early steps of human T cell activation by antigen-presenting cells. J Immunol 1992;**148**:2643–2653.
113. Donnadieu E, Bismuth G, Trautmann A. Antigen recognition by helper T cells elicits a sequence of distinct changes of their shape and intracellular calcium. Curr Biol 1994;**4**:584–595.
114. Negulescu PA, Shastri N, Cahalan MD. Intracellular calcium dependence of gene expression in single T lymphocytes. Proc Natl Acad Sci USA 1994;**91**:2873–2877.
115. Hess SD, Oortgiesen M, Cahalan MD. Calcium oscillations in human T and natural killer cells depend upon membrane potential and calcium influx. J Immunol 1993;**150**:2620–2633.
116. Winslow MM, Neilson JR, Crabtree GR. Calcium signalling in lymphocytes. Curr Opin Immunol 2003;**15**:299–307.

117. Feske S, Giltnane J, Dolmetsch R, Staudt LM, Rao A. Gene regulation mediated by calcium signals in T lymphocytes. Nat Immun 2001;**2**:316–324.
118. Fanger CM, Hoth M, Crabtree GR, Lewis RS. Characterization of T cell mutants with defects in capacitative calcium entry: genetic evidence for the physiological roles of CRAC channels. J Cell Biol 1995;**131**:655–667.
119. Lanzavecchia A, Sallusto F. Progressive differentiation and selection of the fittest in the immune response. Nat Rev Immunol 2002;**2**:982–987.
120. Lewis RS. Calcium signaling mechanisms in T lymphocytes. Annu Rev Immunol 2001;**19**:497–521.
121. Le Deist F, et al. A primary T-cell immunodeficiency associated with defective transmembrane calcium influx. Blood 1995;**85**:1053–1062.
122. Prakriya M, Lewis RS. CRAC channels: activation, permeation, and the search for a molecular identity. Cell Calcium 2003;**33**:311–321.
123. Prakriya M, Lewis RS. Separation and characterization of currents through store-operated CRAC channels and Mg^{2+}-inhibited cation (MIC) channels. J Gen Physiol 2002;**119**:487–507.
124. Nadler MJ, et al. LTRPC7 is a Mg.ATP-regulated divalent cation channel required for cell viability. Nature 2001;**411**: 590–595.
125. Kozak JA, Kerschbaum HH, Cahalan MD. Distinct properties of CRAC and MIC channels in RBL cells. J Gen Physiol 2002;**120**:221–235.
126. Kozak JA, Cahalan MD. MIC channels are inhibited by internal divalent cations but not ATP. Biophys J 2003;**84**:922–927.
127. Fomina AF, Fanger CM, Kozak JA, Cahalan MD. Single channel properties and regulated expression of Ca^{2+} release-activated Ca(2+) (CRAC) channels in human T cells. J Cell Biol 2000;**150**:1435–1444.
128. Chandy KG, Cahalan MD, Pennington M, Norton RS, Wulff H, Gutman GA. Potassium channels in T lymphocytes: toxins to therapeutic immunosuppressants. Toxicon 2001;**39**:1269–1276.
129. Cahalan MD, Wulff H, Chandy KG. Molecular properties and physiological roles of ion channels in the immune system. J Clin Immunol 2001;**21**:235–252.
130. Ghanshani S, et al. Up-regulation of the IKCa1 potassium channel during T-cell activation. Molecular mechanism and functional consequences. J Biol Chem 2000;**275**:37137–37149.
131. Beeton C, et al. A novel fluorescent toxin to detect and investigate Kv1.3 channel up-regulation in chronically activated T lymphocytes. J Biol Chem 2003;**278**: 9928–9937.
132. Beeton C, et al. Selective blockade of T lymphocyte K^+ channels ameliorates experimental autoimmune encephalomyelitis, a model for multiple sclerosis. Proc Natl Acad Sci USA 2001;**98**:13942–13947.
133. Wulff H, et al. The voltage-gated Kv1.3 K^+ channel in effector memory T cells as new target for MS. J Clin Invest 2003;**111**:1703–1713.
134. Pragl B, et al. Synthesis, characterization, and application of cy-dye- and alexa-dye-labeled hongotoxin (1) analogues. The first high affinity fluorescence probes for voltage-gated K^+ channels. Bioconjug Chem 2002;**13**:416–425.
135. Delon J, Bercovici N, Raposo G, Liblau R, Trautmann A. Antigen-dependent and -independent Ca^{2+} responses triggered in T cells by dendritic cells compared with B cells. J Exp Med 1998;**188**:1473–1484.
136. Sykulev Y, Joo M, Vturina I, Tsomides TJ, Eisen HN. Evidence that a single peptide–MHC complex on a target cell can elicit a cytolytic T cell response. Immunity 1996;**4**:565–571.
137. Harding CV, Unanue ER. Quantitation of antigen-presenting cell MHC class II/peptide complexes necessary for T-cell stimulation. Nature 1990;**346**:574–576.
138. Demotz S, Grey HM, Sette A. The minimal number of class II MHC–antigen complexes needed for T cell activation. Science 1990;**249**:1028–1030.
139. Randriamampita C, Boulla G, Revy P, Lemaitre F, Trautmann A. T cell adhesion lowers the threshold for antigen detection. Eur J Immunol 2003;**33**:1215–1223.
140. Dustin ML, Bromley SK, Kan Z, Peterson DA, Unanue ER. Antigen receptor engagement delivers a stop signal to migrating T lymphocytes. Proc Natl Acad Sci USA 1997;**94**:3909–3913.
141. Revy P, Sospedra M, Barbour B, Trautmann A. Functional antigen-independent synapses formed between T cells and dendritic cells. Nat Immun 2001;**2**:925–931.
142. Montes M, McIlroy D, Hosmalin A, Trautmann A. Calcium responses elicited in human T cells and dendritic cells by cell–cell interaction and soluble ligands. Int Immunol 1999;**11**:561–568.
143. Campbell JJ, Butcher EC. Chemokines in tissue-specific and microenvironment-specific lymphocyte homing. Curr Opin Immunol 2000;**12**:336–341.
144. Bargatze RF, Jutila MA, Butcher EC. Distinct roles of L-selectin and integrins alpha 4 beta 7 and LFA-1 in lymphocyte homing to Peyer's patch-HEV in situ: the multistep model confirmed and refined. Immunity 1995;**3**:99–108.
145. Bargatze RF, Butcher EC. Rapid G protein-regulated activation event involved in lymphocyte binding to high endothelial venules. J Exp Med 1993;**178**:367–372.
146. Campbell JJ, Hedrick J, Zlotnik A, Siani MA, Thompson DA, Butcher EC. Chemokines and the arrest of lymphocytes rolling under flow conditions. Science 1998;**279**: 381–384.
147. Pachynski RK, Wu SW, Gunn MD, Erle DJ. Secondary lymphoid-tissue chemokine (SLC) stimulates integrin alpha 4 beta 7-mediated adhesion of lymphocytes to mucosal addressin cell adhesion molecule-1 (MAdCAM-1) under flow. J Immunol 1998;**161**:952–956.
148. Weber C, et al. Specialized roles of the chemokine receptors CCR1 and CCR5 in the recruitment of monocytes and T(H)1-like/$CD45RO^+$ T cells. Blood 2001;**97**: 1144–1146.
149. Campbell JJ, et al. The chemokine receptor CCR4 in vascular recognition by cutaneous but not intestinal memory T cells. Nature 1999;**400**:776–780.
150. Piali L, et al. The chemokine receptor CXCR3 mediates rapid and shear-resistant adhesion-induction of effector T lymphocytes by the chemokines IP10 and Mig. Eur J Immunol 1998;**28**:961–972.
151. Gunn MD, Tangemann K, Tam C, Cyster JG, Rosen SD, Williams LT. A chemokine expressed in lymphoid high endothelial venules promotes the adhesion and chemotaxis of naive T lymphocytes. Proc Natl Acad Sci USA 1998;**95**:258–263.
152. Warnock RA, Campbell JJ, Dorf ME, Matsuzawa A, McEvoy LM, Butcher EC. The role of chemokines in the microenvironmental control of T versus B cell arrest in Peyer's patch high endothelial venules. J Exp Med 2000;**191**:77–88.
153. Stein JV, et al. The CC chemokine thymus-derived chemotactic agent 4 (TCA-4, secondary lymphoid tissue chemokine, 6Ckine, exodus-2) triggers lymphocyte function-associated antigen 1-mediated arrest of rolling T lymphocytes in peripheral lymph node high endothelial venules. J Exp Med 2000;**191**:61–76.
154. Nakano H, et al. Genetic defect in T lymphocyte-specific homing into peripheral lymph nodes. Eur J Immunol 1997;**27**:215–221.
155. Luther SA, Tang HL, Hyman PL, Farr AG, Cyster JG. Coexpression of the chemokines ELC and SLC by T zone stromal cells and deletion of the ELC gene in the plt/plt mouse. Proc Natl Acad Sci USA 2000;**97**:12694–12699.

156. Nakano H, Gunn MD. Gene duplications at the chemokine locus on mouse chromosome 4: multiple strain-specific haplotypes and the deletion of secondary lymphoid-organ chemokine and EBI-1 ligand chemokine genes in the plt mutation. J Immunol 2001;**166**:361–369.
157. Okada T, et al. Chemokine requirements for B cell entry to lymph nodes and Peyer's patches. J Exp Med 2002;**196**:65–75.
158. Gretz JE, Kaldjian EP, Anderson AO, Shaw S. Sophisticated strategies for information encounter in the lymph node: the reticular network as a conduit of soluble information and a highway for cell traffic. J Immunol 1996;**157**:495–499.
159. Gunn MD, Ngo VN, Ansel KM, Ekland EH, Cyster JG, Williams LT. A B-cell-homing chemokine made in lymphoid follicles activates Burkitt's lymphoma receptor-1. Nature 1998;**391**:799–803.
160. Ansel KM, et al. A chemokine-driven positive feedback loop organizes lymphoid follicles. Nature 2000;**406**:309–314.
161. Cyster JG, Ngo VN, Ekland EH, Gunn MD, Sedgwick JD, Ansel KM. Chemokines and B-cell homing to follicles. Curr Top Microbiol Immunol 1999;**246**:87–92 [Discussion 93].
162. Forster R, et al. CCR7 coordinates the primary immune response by establishing functional microenvironments in secondary lymphoid organs. Cell 1999;**99**:23–33.
163. Schweickart VL, et al. Cloning of human and mouse EBI1, a lymphoid-specific G-protein-coupled receptor encoded on human chromosome 17q12-q21.2. Genomics 1994;**23**:643–650.
164. Burgstahler R, Kempkes B, Steube K, Lipp M. Expression of the chemokine receptor BLR2/EBI1 is specifically transactivated by Epstein–Barr virus nuclear antigen 2. Biochem Biophys Res Commun 1995;**215**:737–743.
165. Ngo VN, Tang HL, Cyster JG. Epstein–Barr virus-induced molecule 1 ligand chemokine is expressed by dendritic cells in lymphoid tissues and strongly attracts naive T cells and activated B cells. J Exp Med 1998;**188**: 181–191.
166. Gunn MD, et al. Mice lacking expression of secondary lymphoid organ chemokine have defects in lymphocyte homing and dendritic cell localization. J Exp Med 1999;**189**: 451–460.
167. Foxman EF, Kunkel EJ, Butcher EC. Integrating conflicting chemotactic signals. The role of memory in leukocyte navigation. J Cell Biol 1999;**147**:577–588.
168. Rot A. Neutrophil attractant/activation protein-1 (interleukin-8) induces in vitro neutrophil migration by haptotactic mechanism. Eur J Immunol 1993;**23**: 303–306.
169. Johnston B, Butcher EC. Chemokines in rapid leukocyte adhesion triggering and migration. Semin Immunol 2002;**14**:83–92.
170. Weber KS, von Hundelshausen P, Clark-Lewis I, Weber PC, Weber C. Differential immobilization and hierarchical involvement of chemokines in monocyte arrest and transmigration on inflamed endothelium in shear flow. Eur J Immunol 1999;**29**:700–712.
171. Cinamon G, Shinder V, Alon R. Shear forces promote lymphocyte migration across vascular endothelium bearing apical chemokines. Nat Immunol 2001;**2**:515–522.
172. Palframan RT, et al. Inflammatory chemokine transport and presentation in HEV: a remote control mechanism for monocyte recruitment to lymph nodes in inflamed tissues. J Exp Med 2001;**194**:1361–1373.
173. Gretz JE, Norbury CC, Anderson AO, Proudfoot AE, Shaw S. Lymph-borne chemokines and other low molecular weight molecules reach high endothelial venules via specialized conduits while a functional barrier limits access to the lymphocyte microenvironments in lymph node cortex. J Exp Med 2000;**192**:1425–1440.
174. Middleton J, et al. Transcytosis and surface presentation of IL-8 by venular endothelial cells. Cell 1997;**91**:385–395.
175. Aswanikumar S, Schiffmann E, Corcoran BA, Wahl SM. Role of a peptidase in phagocyte chemotaxis. Proc Natl Acad Sci USA 1976;**73**:2439–2442.
176. Malchow D, Gerisch G. Short-term binding and hydrolysis of cyclic-3′: 54′-adenosine monophosphate by aggregating Dictyostelium cells. Proc Natl Acad Sci USA 1974;**71**:2423–2427.
177. Yuli I, Snyderman R. Extensive hydrolysis of N-formyl-L-methionyl-L-leucyl-L-[3H] phenylalanine by human polymorphonuclear leukocytes. A potential mechanism for modulation of the chemoattractant signal. J Biol Chem 1986;**261**:4902–4908.